

# Cytochrome $bc_1$ Complex [2Fe-2S] Cluster and Its Interaction with Ubiquinone and Ubiquinol at the $Q_o$ Site: A Double-Occupancy $Q_o$ Site Model<sup>†</sup>

Huangen Ding,<sup>\*,‡</sup> Dan E. Robertson,<sup>‡</sup> Fevzi Daldal,<sup>§</sup> and P. Leslie Dutton<sup>‡</sup>

The Johnson Research Foundation, Department of Biochemistry and Biophysics and Department of Biology, University of Pennsylvania, Philadelphia, Pennsylvania 19104

Received July 3, 1991; Revised Manuscript Received December 23, 1991

**ABSTRACT:** The ubiquinone complement of *Rhodobacter capsulatus* chromatophore membranes has been characterized by its isooctane solvent extractability and electrochemistry; we find that the main ubiquinone pool ( $Q_{pool}$ ) amounts to about 80% of the total ubiquinone and has an  $E_{m7}$  value close to 90 mV. To investigate the interactions of ubiquinone with the cyt  $bc_1$  complex, we have examined the distinctive EPR line shapes of the [2Fe-2S] cluster of the cyt  $bc_1$  complex when the  $Q_{pool}$ –cyt  $bc_1$  complex interactions are modulated by changing the numbers of Q or  $QH_2$  present (by solvent extraction and reconstitution), by the exposure of the [2Fe-2S] to the  $Q_{pool}$  in different redox states, by the presence of inhibitors specific for the  $Q_o$  site (myxothiazol and stigmatellin) and  $Q_i$  site (antimycin), and by site-specific mutations of side chains of the cyt  $b$  polypeptide (mutants F144L and F144G) previously identified as important for  $Q_o$  site structure. Evidence suggests that the  $Q_o$  site can accommodate two ubiquinone molecules. One (designated  $Q_{os}$ ) is bound relatively strongly and is second only to the ubiquinone of the  $Q_A$  site of the reaction center in its resistance to solvent extraction. In this strong interaction, the  $Q_o$  site binds Q and  $QH_2$  with approximately equal affinities. Their bound states are distinguished by their effects on the [2Fe-2S] cluster spectral feature at  $g_x$  at 1.783 (Q) and  $g_x$  at 1.777 ( $QH_2$ ); titration of the line-shape change reveals an  $E_{m7}$  value of approximately 95 mV. The other molecule ( $Q_{ow}$ ) is bound more weakly, in the same range as the ubiquinone of the  $Q_B$  site of the reaction center. Again, the affinities of the Q form ( $g_x$  at 1.800) and  $QH_2$  form ( $g_x$  at 1.777) are nearly equal, and the  $E_{m7}$  value measured is approximately 80 mV. These results are discussed in terms of earlier EPR analyses of the cyt  $bc_1$  complexes of other systems. A  $Q_o$  site double-occupancy model is considered that builds on the previous model based on  $Q_o$  site mutants [Robertson, D. E., Daldal, F., & Dutton, P. L. (1990) *Biochemistry* 29, 11249–11260] and includes the recent suggestion that two of the [2Fe-2S] cluster ligands of the *R. capsulatus* cyt  $bc_1$  complex are histidines [Gurbiel, R. J., Ohnishi, T., Robertson, D. E., Daldal, F., & Hoffman, B. M. (1991) *Biochemistry* 30, 11579–11584]. We speculate that the cyt  $bc_1$  complex completes a full enzymatic turnover without necessary exchange of ubiquinone with the  $Q_{pool}$ .

The cytochrome  $bc_1$  complex (ubiquinol–cytochrome  $c$  oxidoreductase) is a redox protein complex common to both respiratory and photosynthetic systems. In respiration, the complex receives electrons from NADH, succinate, and other substrates via the ubiquinone pool ( $Q_{pool}$ ) and donates electrons, via cyt  $c$ , to cyt  $c$  oxidase and thence to dioxygen. In photosynthetic bacteria, the cyt  $bc_1$  complex participates in a light-driven cyclic system with the reaction center protein, again linked via the  $Q_{pool}$  and a cyt  $c$ .

The cyt  $bc_1$  complex is an intrinsic membrane protein that uses the redox potential difference of approximately 250 mV between the  $Q_{pool}$  and cyt  $c$  to drive the separation of charge and movement of protons across the supporting membrane. Its structure includes three subunits, one containing a [2Fe-2S] cluster, one a cytochrome  $c_1$ , and one containing two cytochromes  $b$  (designated  $b_H$  and  $b_L$ , according to their relatively high and low redox midpoint potentials) [for reviews, see Crofts and Wraight (1983), Rich (1984), Dutton (1986), Jackson (1988), Cramer and Knaff (1989), and Prince (1990)]. The cyt  $bc_1$  complex also accommodates two distinct sites for the

redox reactions of the ubiquinone pool; these are designated  $Q_o$  and  $Q_i$  [Mitchell, 1975, 1976; for recent citations, see Robertson and Dutton (1988)].

The  $Q_o$  site is located near the periplasmic side of the bacterial cytoplasmic membrane (Glaser & Crofts, 1984; Robertson & Dutton, 1988), where it catalyzes the two-electron oxidation of ubiquinol ( $QH_2$ ) to ubiquinone (Q). This oxidation reaction involves the cooperation of two one-electron redox centers, namely, the [2Fe-2S] cluster and cyt  $b_L$ , both of which are considered to be closely positioned to the  $Q_o$  site (Robertson & Dutton, 1988; Robertson et al., 1990). The  $Q_o$  site is generally accepted to perform two separate, serial  $QH_2$  oxidations in order to complete a full turnover of the cyt  $bc_1$  complex (Crofts et al., 1983). An important part of the definition of the  $Q_o$  site is the idea that the cyt  $bc_1$  complex inhibitors stigmatellin and myxothiazol bind stoichiometrically and specifically to the  $Q_o$  site and impede  $QH_2$  oxidation. These inhibitors are used throughout this report to aid in the identification of events that are operationally linked to the  $Q_o$  site.

<sup>†</sup> Research support is acknowledged from PHS Grants GM27302 (to P.L.D.) and GM 38237 (to F.D.).

<sup>\*</sup> Address correspondence to this author at the Johnson Research Foundation, Department of Biochemistry and Biophysics, B501 Richards Building, The University of Pennsylvania, 37th and Hamilton Walk, Philadelphia, PA 19104.

<sup>‡</sup> Department of Biochemistry and Biophysics.

<sup>§</sup> Department of Biology.

<sup>1</sup> Abbreviations: cyt, cytochrome; cyt  $bc_1$  complex, ubiquinol–cytochrome  $c$  oxidoreductase; Q, ubiquinone;  $QH_2$ , ubiquinol; cyt  $b_L$ , low potential cyt  $b_{566}$  of cyt  $bc_1$ ; cyt  $b_H$ , high potential cyt  $b_{560}$  of cyt  $bc_1$ ;  $Q_o$  site, ubiquinol oxidizing site;  $Q_i$  site, ubiquinol reducing site; EPR, electron paramagnetic resonance; UHDBT, 5-undecyl-6-hydroxy-4,7-dioxobenzothiazol; HMQQ, 7-(*n*-heptadecyl)mercapto-6-hydroxy-5,8-quinolinequinone; DMSO, dimethyl sulfoxide;  $E_{m7}$ , electrochemical midpoint potential at pH 7.0.

The other ubiquinone binding site, the *Q*<sub>i</sub> site, is located near cyt *b*<sub>H</sub> and close to the cytoplasmic side of the membrane (Robertson & Dutton, 1988), where its redox chemistry (Ohnishi & Trumpower, 1980; DeVries et al., 1982b; Robertson et al., 1984; Salerno et al., 1990) indicates that it can catalyze the net reduction of *Q* to *QH*<sub>2</sub> in two separate, one-electron reduction steps in a way most likely analogous to that of the well-described *Q*<sub>B</sub> site of the photosynthetic reaction center from bacteria (Wraight, 1979; Vermeglio & Clayton, 1977) and green plant photosystem II (Crofts & Wraight, 1983; Jackson, 1988; Cramer & Knaff, 1989; Prince, 1990). Antimycin interacts at the *Q*<sub>i</sub> site with high affinity and specificity, independent of the presence of *Q*<sub>o</sub> site inhibitors (van den Berg et al., 1979; Von Jagow & Link, 1986). Hence, antimycin is a useful agent in operationally identifying reactions associated with the *Q*<sub>i</sub> site.

At present, little is known about the affinities of the *Q*<sub>i</sub> and *Q*<sub>o</sub> sites of the cyt *bc*<sub>1</sub> complex and the *Q*<sub>B</sub> site of the reaction center for *Q* and *QH*<sub>2</sub> of the *Q*<sub>pool</sub>. Moreover, it is uncertain whether the sites are mainly unoccupied or occupied under physiological conditions, whether the sites have any significant preference for binding of *Q* or *QH*<sub>2</sub> of the *Q*<sub>pool</sub>, or how many *Q* or *QH*<sub>2</sub> molecules can be accommodated by each of the sites. An opportunity to approach these problems for the cyt *bc*<sub>1</sub> complex *Q*<sub>o</sub> site is provided by the closely associated [2Fe-2S] cluster. The EPR line shape of the [2Fe-2S] cluster in the cyt *bc*<sub>1</sub> complex is sensitive to the redox state of the *Q*<sub>pool</sub> (Siedow et al., 1978; DeVries et al., 1982a; Matsuura et al., 1983), and evidence has accrued that the *Q*/*QH*<sub>2</sub> interaction with the [2Fe-2S] cluster might occur through specific interactions with residues at the *Q*<sub>o</sub> site (Robertson et al., 1990). In addition, it is evident that the *Q*<sub>o</sub> site inhibitors, stigmatellin and myxothiazol, interact in some way with the [2Fe-2S] cluster to induce their own EPR spectral signatures (DeVries et al., 1983; Ohnishi et al., 1988; McCurley et al., 1990). Thus, the [2Fe-2S] cluster line shape lends itself to the exploration of the thermodynamics of the *Q*<sub>o</sub> site occupancy.

In this report, we describe the use of the cyt *bc*<sub>1</sub> complex from the photosynthetic bacterium *R. capsulatus* to investigate the [2Fe-2S] cluster's EPR spectrum as a function of the redox state of the *Q*<sub>pool</sub>, varied by redox potentiometry, and as a function of the number of ubiquinones present in the *Q*<sub>pool</sub> modulated by solvent extraction and reconstitution [see also DeVries et al. (1982a) and Takamiya et al. (1979b)]. We have also examined and made use of the [2Fe-2S] cluster line shape in reporting interactions between [2Fe-2S] and the *Q*<sub>o</sub> and *Q*<sub>i</sub> site inhibitors and with ubiquinone in selected *Q*<sub>o</sub> site mutants. The experiments clarify some of the previous views, which were clouded by reports of heterogeneity in the [2Fe-2S] cluster line shape (DeVries et al., 1979; Hagen et al., 1985; Meinhardt et al., 1987) and suggest that the *Q*<sub>o</sub> site is more elaborate than previously considered. These results indicate that the *Q*<sub>o</sub> site accommodates two ubiquinone molecules and suggest a simple model in which the cyt *bc*<sub>1</sub> complex can perform a complete turnover without the exchange of ubiquinone with the *Q*<sub>pool</sub>.

## MATERIALS AND METHODS

In this report, cells of a cyt *bc*<sub>1</sub> overproducing mutant of *R. capsulatus*, pMT0-404/MT-RKB1, containing increased amounts of cyt *bc*<sub>1</sub> complex per total amount of membrane protein (Atta-Asafo-Adjei & Daldal, 1991) were used. A detailed description of the cyt *bc*<sub>1</sub> complex overproducer strains will be reported elsewhere (Tokito and Daldal, manuscript in preparation). The bacteria displayed normal growth rates when illuminated under anaerobic conditions; the cyt *b* site-directed mutants F144G and F144L (Tokito and Daldal,

manuscript in preparation) were also grown under these conditions. Cells were harvested during the late log phase (typically, 24 h after a ~5% inoculum) and were used immediately. Chromatophores were prepared as described previously (Dutton et al., 1975). Redox potentiometry was performed using methods and equipment described in Dutton (1978).

Light-harvesting bacteriochlorophyll was measured according to Clayton (1963). The reaction center concentration was determined from the flash-activated absorbance change of its bacteriochlorophyll dimer (forming [*BChl*]<sub>2</sub><sup>+</sup>) at 605 nm minus 540 nm in chromatophores poised at high redox potentials so that the cytochrome *c*<sub>2</sub> was oxidized before activation (Dutton et al., 1975). With the cytochrome *c*<sub>2</sub> oxidized, the flash generated [*BChl*]<sub>2</sub><sup>+</sup> is stable for milliseconds and is readily measured.

After solvent extraction of ubiquinone (see below), the occupancy of the reaction center *Q*<sub>A</sub> site by remaining ubiquinone was measured by its obligate role in the stable flash generation of [*BChl*]<sub>2</sub><sup>+</sup> (Okamura et al., 1975) as described above; hence, comparison of the amplitude of flash-generated [*BChl*]<sub>2</sub><sup>+</sup> in extracted chromatophores with that in unextracted chromatophores provides a reliable measure of *Q*<sub>A</sub> site occupancy. The occupancy by ubiquinone of the *Q*<sub>B</sub> site was determined from the time course of flash-generated [*BChl*]<sub>2</sub><sup>+</sup> reduction under the same conditions but with added antimycin and myxothiazol to block any reduction of the [*BChl*]<sub>2</sub><sup>+</sup> via the cyt *bc*<sub>1</sub> complex. In this assay, the fraction of the slow [*BChl*]<sub>2</sub><sup>+</sup> reduction phase (0.85/s) signals ubiquinone in the *Q*<sub>B</sub> site; this was resolved from the faster reduction phase (14.4/s) which signals no ubiquinone in the *Q*<sub>B</sub> site, according to a curve fitting program (C. C. Moser, unpublished) using the nonlinear least-squares procedures of Bevington (1969). It is noted that this method only provides an upper limit for the level of *Q*<sub>B</sub> site occupancy at equilibrium, since any ubiquinone entering the *Q*<sub>B</sub> site during the rather long lifetime of the activated state ([*BChl*]<sub>2</sub><sup>+</sup>*Q*<sub>A</sub><sup>-</sup> state, decaying at 14.4/s) will be seen as an occupant.

The cyt *bc*<sub>1</sub> complex content of the chromatophores from the overproducing mutant pMT0-404/MT-RKB1 chosen for this work was determined by the antimycin titration method as previously described (van den Berg et al., 1979) and expressed as a ratio with the reaction center under photosynthetic growth conditions. In the chromatophores of cells grown as described above, we found the cyt *bc*<sub>1</sub> complex:reaction center ratio in the overproducing strain to be approximately 0.6, a value similar to that of the wild-type strain MR126 (Robertson et al., 1986). This finding, therefore, leads to the conclusion that this strain also contains elevated amounts of the reaction center. However, it appears that the overproduction of these redox proteins does not extend to the light-harvesting bacteriochlorophyll pigment proteins (LH proteins). The level of the bacteriophyll was lowered to values typically around 150 instead of the 250 per reaction center found in the wild-type strain grown similarly.

Extraction of ubiquinone from the membranes was performed on lyophilized chromatophores using isooctane or on aqueous suspensions using methanol-acetone on the basis of the methods previously described (Takamiya & Dutton, 1979). Briefly, the methods were as follows:

(a) *Isooctane Extraction.* Stepwise removal of ubiquinone from chromatophores involved cycles of extraction by dry isooctane, for a limited period of time, of material (about 1 g dry weight) dried onto the surface of a 250-mL flask in a Virtis lyophilizer. We found that repeated gentle swirling at

room temperature for 30 min with 700 mL of dry isooctane reduced the  $Q_{\text{pool}}$  size to near-zero in four or five steps, convenient for the purposes of the present work. When more completely extracted material was required, one or two cycles were performed but with prolonged extraction, usually for several hours.

It should be mentioned that we do not fully understand the extraction process. The removal is clearly severely rate-limited (i.e., the solvent is in large excess and not limiting on a solubility or partitioning basis), and experience suggests that the efficiency for a near complete removal may be affected by atmospheric humidity. Nevertheless, variability is within useful limits, and the effects of a given extraction regimen are acceptably reproducible. One example of the time course of extraction of ubiquinone from similar membranes has been presented (Venturoli et al., 1986).

After completion of a chosen number of isooctane extraction cycles, the ubiquinone remaining was assayed after further extraction with acetone-methanol; this solvent mixture removes all ubiquinones as described in section b, below.

The extraction process is reversible (Baccarini-Melandri et al., 1982). Reconstitution of extracted chromatophores (200 mg of dried material, which typically contains 75 nmol of reaction center) was performed through suspension in 10 mL of isooctane containing ubiquinone-10 (Sigma, St. Louis, MO) to deliver the required Q per reaction center molar ratio, followed by slow drying in a rotary evaporator at room temperature. This method is only semiquantitative, since the final distribution of added ubiquinone in the chromatophores is not known. However, addition of low or high amounts of ubiquinone provided chromatophores with properties consistent with the presence of a small or large  $Q_{\text{pool}}$ , respectively.

(b) *Acetone-Methanol Extraction.* The total ubiquinone content of chromatophores was determined by extraction of the aqueous suspension through the addition of a 10-fold excess of 1:1 acetone-methanol (v/v) solvent mixture, followed by separation of the ubiquinone from pigments through extraction with petroleum ether (35–60 °C) and washing with 95% (v/v) methanol (Kröger & Klingenberg, 1973). Chromatophores were analyzed in this way to determine the total ubiquinone content or the amount of ubiquinone remaining after each isooctane extraction.

This latter method of extraction was also used in redox titrations of the ubiquinone of *Rhodobacter sphaeroides* chromatophores as previously described (Takamiya & Dutton, 1979). Quenching the chromatophores with cold acetone-methanol is known to trap the Q and  $QH_2$  populations in the proportions prevailing in the electrochemically poised system (Kröger & Klingenberg, 1973).

Quantitation of extracted ubiquinone was performed spectrophotometrically in duplicate after taking up the dried ubiquinone extract in absolute ethanol using the ferric chloride-oxidized minus borohydride-reduced extinction coefficient  $14 \text{ mM}^{-1} \text{ cm}^{-1}$  at 275 nm (Barr & Crane, 1971); variations in the duplicate measurements were within 10%. In the redox titrations, the percentage  $QH_2$  in the extract was determined by the difference in the absorbance at 275 nm before and after the addition of a few crystals of solid borohydride, freshly removed from the container. Q and  $QH_2$  levels of the chromatophore were related to the photosynthetic reaction center protein content, which was taken to be the primary standard, since its concentration can be assayed directly and reliably.

EPR measurements were carried out on a Varian E-109 X-band spectrometer equipped with a flowing helium cryostat (Air Products LTD3-110). EPR conditions: temperature, 20

K; microwave power, 2 mW; modulation amplitude, 1.25 mT; modulation frequency, 100 kHz; microwave frequency 9.31 GHz; time constant, 0.25 s; scan rate,  $25 \text{ mT min}^{-1}$ . EPR spectra were averaged using an IBM personal computer interfaced to the E-109 EPR spectrometer. We thank Dr. Tomoko Ohnishi for making her software available to us for the manipulations of the EPR spectra.

## RESULTS

### *Characterization of the $Q_{\text{pool}}$ of *R. capsulatus* Chromatophore Membranes*

(a) *Quantitative Analysis of Ubiquinone in the Cyt  $bc_1$  Complex Overproducing Mutant.* We have determined that there are  $32 \pm 8$  ( $N = 3$ ) ubiquinone molecules per reaction center in the chromatophore membrane of the overproducer strain pMT0-404/MT-RKB1 of *R. capsulatus* when grown photoheterotrophically and harvested in late log phase after 24 h. This compares to 26 ubiquinones per reaction center from *R. capsulatus* strain MR 126 (Robertson et al., 1983) and  $25 \pm 3$  (Takamiya & Dutton, 1979) or 25 (Venturoli et al., 1986) in *R. sphaeroides* strain GA when grown similarly. We consider that the differences in ubiquinone content between wild-type or cyt  $bc_1$ -overproducing strains are of little significance, and, for the experiments reported here, the differences are not great enough to affect the measurements or conclusions.

Redox titrations show that 80% of the ubiquinone in the chromatophore membranes yields an  $E_{m7}$  value of  $90 \pm 6 \text{ mV}$  ( $N = 2$ ), identifiable as the  $Q_{\text{pool}}$ . The remaining 20% of the ubiquinone population, amounting to five to six ubiquinones per reaction center, is not reduced at redox potentials as low as  $-90 \text{ mV}$ , suggesting that the members of this population have much lower redox potentials; the identities of ubiquinone in this population are currently uncertain. Similar observations have been made in earlier work on *R. sphaeroides* (Takamiya & Dutton, 1979). Likewise, 80% of the 15 ubiquinones per cyt  $bc_1$  complex in beef heart mitochondria were shown to comprise the  $Q_{\text{pool}}$  with an  $E_{m7}$  value in the 50–100 mV range, while 20% were part of an unidentified low-potential population (Urban & Klingenberg, 1969; Kröger & Klingenberg, 1973).

(b) *Solvent Extraction Characteristics.* The first cycle of isooctane extraction typically removes 70–80% of the total ubiquinone, yielding chromatophores with five to seven ubiquinones per reaction center. The next two or three cycles lower the number of ubiquinones remaining to about two per reaction center. One of the two can usually be removed in further (either one or two) extraction cycles, but the final one, identified as the ubiquinone in the  $Q_A$  site of the reaction center (see Materials and Methods for details and later for analysis), is refractory to extraction by the present protocol.

### *The Response of the [2Fe-2S] Cluster EPR Spectrum to the Occupancy of the $Q_o$ Site*

(a) *Redox State of the  $Q_{\text{pool}}$ .* The  $E_{m7}$  value of the [2Fe-2S] cluster in *R. capsulatus* is approximately 290 mV (Prince et al., 1975; Robertson et al., 1986), and, therefore, poisoning the redox potential of the chromatophore suspension below 200 mV (at pH 7.0) establishes the [2Fe-2S] cluster over 90% in the reduced, paramagnetic form. In Figure 1A, spectrum a was taken at a redox potential of 200 mV (pH 7.0), where the  $Q_{\text{pool}}$  is essentially in the fully oxidized Q form. Under these conditions, the EPR spectrum of the [2Fe-2S] cluster is characterized by sharp transitions at  $g_z$  2.019 (not shown),  $g_y$  1.890, and  $g_x$  1.800. Figure 1B, spectrum a, was taken at a redox potential of 0 mV (pH 7.0), which establishes the  $Q_{\text{pool}}$

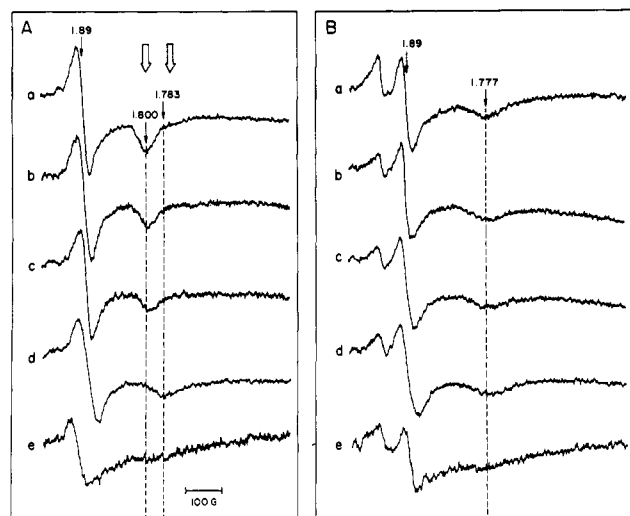


FIGURE 1: EPR spectra of the [2Fe-2S] cluster of the *R. capsulatus* cyt *bc*<sub>1</sub> complex when the  $Q_{\text{pool}}$  is extracted in a stepwise manner. The chromatophores were suspended at pH 7.0, to 25  $\mu\text{M}$  reaction center, poised at 200 mV (panel A), or reduced with a limited amount of sodium dithionite (panel B). The presence of (a) 2.5, (b) 7.0, (c) 4.1, (d) 2.2, and (e) 1.1 ubiquinones per reaction center was obtained after (a) no extraction or after subtraction to (b) one, (c) two, (d) three, and (e) five extraction cycles. Spectrum e in panels A and B is another preparation containing the same reaction center concentration.  $g$  values are indicated on the peak of each spectrum. The open arrows pertain to further analysis, described later in the legend to Figure 5 and Table I.

in an essentially fully reduced  $\text{QH}_2$  form. Under these conditions, the [2Fe-2S] EPR spectrum is broadened overall,  $g_x$  and  $g_y$  appear at 2.020 and 1.890, respectively, and the clearly shallower  $g_x$  band appears at 1.777.

Thus, the line shapes for the [2Fe-2S] cluster of the *R. capsulatus* cyt *bc*<sub>1</sub> complex are distinctly different when the  $Q_{\text{pool}}$  is fully reduced or oxidized. Similar results have been reported in many other systems (Siedow et al., 1978; DeVries et al., 1979; Yang & Trumpower, 1986; Andrews et al., 1990). The simplest interpretation of these effects is that, when they are bound in the  $Q_o$  site, Q and  $\text{QH}_2$  interact differently with the adjacent [2Fe-2S] cluster.

(b) *The Effect of Stepwise Ubiquinone Extraction.* Figure 1 also shows the effect on the line shape of the [2Fe-2S] cluster as the  $Q_{\text{pool}}$  size is diminished in steps by isooctane extraction to a level close to approximately one ubiquinone per reaction center. As was mentioned above, the last remaining ubiquinone to be extracted is predominantly the  $Q_A$  molecule, and, hence, ubiquinone available for other sites approaches zero. Spectra were obtained when the ubiquinone remaining was either fully oxidized (Q form; panel A) or fully reduced ( $\text{QH}_2$  form; panel B).

Figure 1A shows that, down to 7.0 Q per reaction center (spectrum b), there is little or no change in the line shape. At 4.1 Q per reaction center (spectrum c), there is minor diminution of the amplitudes of the  $g_y$  at 1.890 and the  $g_x$  at 1.800 and the appearance of a small shoulder on its high field side. At 2.2 Q per reaction center (spectrum d), the  $g_y$  amplitude again diminishes only to a minor degree, but there is a substantial loss of amplitude at  $g_x$  1.800, and the high field shoulder of the  $g_x$  is now dominant with a position close to 1.783.

At 1.1 ubiquinone molecules per reaction center (spectrum e), the [2Fe-2S] line shape is different again. Of these 1.1 ubiquinones remaining, 85% are accounted for by the  $Q_A$  site (see Materials and Methods), leaving only approximately 0.25 ubiquinone molecules per reaction center potentially available

for other sites. The EPR line shape of the [2Fe-2S] cluster in this extensively extracted material is broadened considerably beyond that seen in the presence of Q or  $\text{QH}_2$ . The shallowness of the associated  $g_x$ , in addition to possible interference from any residual contributions from the state with the more pronounced  $g_x$  at 1.783, makes it difficult to assign an accurate  $g$  value. We estimate the  $g_x$  of the [2Fe-2S] cluster in the absence of ubiquinone to be in the region of 1.765 and propose that this spectrum approximates the [2Fe-2S] cluster in an environment devoid of Q. The loss of the  $g_x$  at 1.783 as the total number of Q molecules per reaction center decreases from 2.2 to 1.1 suggests that the Q penultimately extracted from the chromatophore is responsible for a form of [2Fe-2S] cluster characterized by a  $g_x$  at 1.783.

Figure 1B shows spectra obtained with the same material as used in Figure 1A except that the chromatophores were poised with  $Q_{\text{pool}}$  reduced prior to freezing. Once again, the removal of  $Q_{\text{pool}}$  (in the  $\text{QH}_2$  form) down to 7.0  $\text{QH}_2$  per reaction center (spectrum b) has little effect on the [2Fe-2S] line shape; the characteristic feature,  $g_x$  at 1.777, remains. In contrast to the data shown in Figure 1A with 2.2 Q per reaction center, the spectrum of a preparation with 2.2  $\text{QH}_2$  per reaction center is not distinctly different from those with larger amounts of  $\text{QH}_2$ . Thus, from 7.0 to 2.2  $\text{QH}_2$  per reaction center (spectra b–d), the major EPR spectral response analogous to the  $g_x$  1.800/1.783 transition seen for Q is not encountered.

However, on changing the  $\text{QH}_2$  level from 2.2 to 1.1 per reaction center (spectra d–e), there is a detectable change, yielding a spectrum similar to that shown at 1.1 Q per reaction center. This result is consistent with the idea that, at this very low ubiquinone level, the [2Fe-2S] cluster spectrum assumes a line shape characteristic of the absence of ubiquinone in the  $Q_o$  site. The finding that the line shape is the same at 200 and 0 mV for the exhaustively extracted material supports the conclusion that the changes in the line shape seen in the presence of sufficient  $Q_{\text{pool}}$ , poised oxidized or reduced, result specifically from interactions of Q and  $\text{QH}_2$  with the [2Fe-2S] cluster. Thus, these changes probably are not derived from other redox-linked reactions in the cyt *bc*<sub>1</sub> complex or from the mediating dyes used in the potentiometry (also see Figure 6E).

In summary, we have identified two distinct interactions of Q with the [2Fe-2S] cluster. One, evident at high Q levels, is characterized by the  $g_x$  at 1.800 and appears similar to those reported before in a variety of systems. The other, evident when as few as one available Q remains associated with the cyt *bc*<sub>1</sub> complex, is characterized by the  $g_x$  at 1.783 and appears to be novel. The interaction of the [2Fe-2S] cluster with  $\text{QH}_2$  is characterized by its  $g_x$  at 1.777 and, from the work thus far, does not clearly reveal more than one spectral form dependent on the amount of  $\text{QH}_2$ . Finally, a different spectrum is recognized that is indicative of a [2Fe-2S] cluster interacting with an environment free of Q or  $\text{QH}_2$ ; this spectrum is very broad, and, although difficult to measure, its shallow  $g_x$  appears to be at 1.765.

(c) *Reconstitution.* Figure 2 shows that the chromatophore extraction procedure is reversible. Exhaustively extracted material (spectrum a) was reconstituted with ubiquinone-10 and poised at 200 mV so that any ubiquinone added was in the Q form. Figure 2, spectrum b, shows that reconstitution of chromatophores with a total of 1.7 Q added per reaction center reestablishes the features (Figure 1A, spectrum d) of the state seen at Q levels between 1.1 and 4.1 Q per reaction center with  $g_x$  at 1.783. This state was difficult to achieve

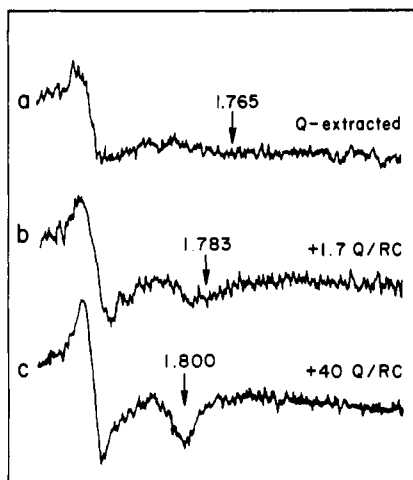


FIGURE 2: Reconstitution of the EPR spectra of the [2Fe-2S] cluster of the *R. capsulatus* cyt *bc*<sub>1</sub> complex in isooctane-extracted chromatophores. Chromatophores containing about 20  $\mu$ M reaction center were poised at near 200 mV (pH 7.0). Spectrum a is the EPR spectrum of the chromatophores extracted extensively with isooctane to 0.8 Q per reaction center; spectrum b was obtained after 1.7 ubiquinone-10 per reaction center was added to the extracted chromatophores; spectrum c was obtained after 40 ubiquinone-10 per reaction center was added to the extracted chromatophores.

without substantial contribution from the  $g_x$  at 1.800 seen at higher Q levels. However, adding Q in the region of 1.7 Q per reaction center was found reliably to yield some, but not optimal, amounts of the  $g_x$  at 1.783 state without significant contributions from the  $g_x$  at 1.800 state. Figure 2, spectrum c, shows that reconstitution with 40 Q added per reaction center reestablish the native spectrum, as shown in Figure 1A, spectrum a. The amplitudes of  $g_y$  and  $g_x$  in the reconstituted sample are about 90% those of unextracted material. This demonstrates that the general broadening of the [2Fe-2S] EPR spectrum as in Figure 1, spectrum e, and Figure 2, spectrum a, is mainly due to the empty  $Q_o$  site, not to the loss of [2Fe-2S] cluster spins after ubiquinone extraction. Likewise, although not shown, addition of 40 Q to the material initially displaying the  $g_x$  at 1.783 (achieved by extraction) also reestablishes the native spectrum with  $g_x$  at 1.800. It is also important to mention that the native millisecond turnover of cyt *bc*<sub>1</sub> complex after flash activation in ubiquinone-extracted chromatophores is fully recovered after reconstitution with ubiquinone-10 (data not shown), as described by Takamiya and Dutton (1979) and Venturoli et al. (1986).

The success of the reconstitution of the key spectra of the [2Fe-2S] cluster in chromatophores strengthens the suggestion that the observed line-shape alterations are the result of ubiquinone-specific interactions and argues against the possibility that they are effects of structural changes caused by depletion of other compounds, such as membrane lipids.

**(d) Effect of  $Q_o$  Site Mutations on [2Fe-2S] Cluster- $Q$  Interactions.** Figure 3 compares [2Fe-2S] cluster EPR spectra of pMT0-404/MT-RKB1 with two  $Q_o$  site mutants of *R. capsulatus*, in which phenylalanine (F) in the position 144 of the cyt *b* polypeptide has been replaced with glycine (F144G) or leucine (F144L) (Tokito and Daldal, manuscript in preparation). The  $Q_o$  site-catalyzed  $QH_2$  oxidation reaction is impaired in these mutants, being slowed approximately 15-fold in F144L (Robertson et al., 1990) and 4-fold in F144G (Ding et al., manuscript in preparation). The [2Fe-2S] cluster EPR spectra of F144L [Figure 3, spectrum c, and Robertson et al. (1990)] and also of another mutant, G158D [see Robertson et al. (1990)], two severely impaired mutants, are similar to each other and, also, to those shown in Figure 1A, spectrum

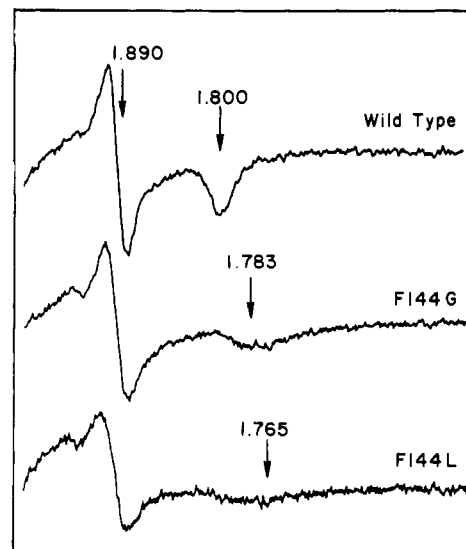


FIGURE 3: EPR spectra of the [2Fe-2S] cluster of the *R. capsulatus* cyt *bc*<sub>1</sub> complex of selected  $Q_o$  site mutants. Chromatophores containing 20  $\mu$ M reaction center of wild-type and mutant strains were poised at a redox potential of 200 mV, pH 7.0. The EPR spectra of the [2Fe-2S] cluster in (a) wild-type and (b) F144G and (c) F144L mutants of the cyt *b* polypeptide are presented.

e, and Figure 1B, spectrum e, for exhaustively extracted chromatophores. Additionally, the mutant spectra are insensitive to the redox state of the large  $Q_{pool}$  present [not shown, but see Figure 5 in Robertson et al. (1986) and Figure 4 in Robertson et al. (1990) for the G158D mutant], consistent with the idea that the  $Q_o$  sites of F144L and G158D have affinities for Q and  $QH_2$  lowered sufficiently to render the  $Q_o$  site empty of these molecules. In contrast, the analogous [2Fe-2S] cluster EPR spectrum for the marginally impaired mutant, F144G, displays a line shape similar to that with the novel  $g_x$  at 1.783, shown for the chromatophores partially extracted to 2.2 Q per reaction center (Figure 1A, spectrum d) and for the chromatophores reconstituted by 1.7 Q per reaction center (Figure 2, spectrum b).

The reproduction of [2Fe-2S] cluster EPR spectra and their redox potential independence in chromatophores of unextracted but severely dysfunctional mutants (F144L and G158D) provides support for the idea that the [2Fe-2S] cluster, in the exhaustively extracted wild-type strain, is in a state that approaches that when the associated  $Q_o$  site is devoid of ubiquinone. Likewise, the reproduction of the novel [2Fe-2S] cluster spectrum, with  $g_x$  at 1.783 in a marginally impaired but unextracted mutant (F144G), adds considerable confidence to the suggestion that this is a bona fide form of the [2Fe-2S] cluster, induced in this case by interaction of the [2Fe-2S] cluster with a  $Q_o$  site of lowered affinity in the presence of a native-sized  $Q_{pool}$ .

**(e) The Effect of Inhibitors Specific to the  $Q_o$  and  $Q_i$  Sites.** It has been established that the addition of myxothiazol (von Jagow & Engle, 1981; DeVries et al., 1983; Meinhardt & Crofts, 1982) or stigmatellin (von Jagow & Ohnishi, 1985) to stoichiometric equivalence with the cyt *bc*<sub>1</sub> complex causes complete inhibition of  $Q_o$  site function. Spectra a and b in Figure 4 show control chromatophores with either native levels of 26 Q per reaction center or, after partial extraction, close to 2 Q per reaction center (as in Figure 1A, spectrum d). These display the expected [2Fe-2S] cluster spectra characterized by  $g_x$  at 1.800 and 1.783, respectively. The spectra of Figure 4 show how these line shapes are altered in the presence of stigmatellin (parts c and d) or myxothiazol (parts e and f), respectively, added to levels in slight stoichiometric

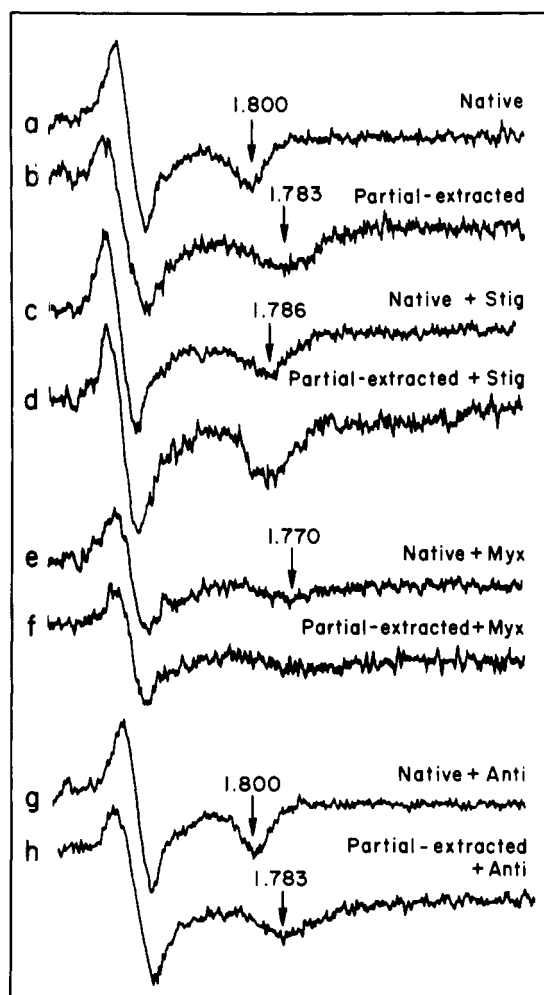


FIGURE 4: Comparison of the EPR spectra of the [2Fe-2S] cluster of the *R. capsulatus* cyt *bc*<sub>1</sub> complex, between partially extracted and native  $Q_{\text{pool}}$  chromatophores in the presence of  $Q_0$  and  $Q_1$  site inhibitors. Chromatophores, suspended to 20  $\mu\text{M}$  reaction center with native ubiquinone levels (26 Q per reaction center) and partially extracted  $Q_{\text{pool}}$  (close to 2 Q per reaction center), were poised at a redox potential of 200 mV (pH 7.0). The effects on spectra at 26 and 2 Q per reaction center (a and b, respectively) are shown when the inhibitors stigmatellin (c and d), myxothiazol (e and f), and antimycin A (g and h) are added at a ratio of 0.7 per reaction center (i.e., 1.2 per cyt *bc*<sub>1</sub> complex). The inhibitors were added from DMSO stock solution.

excess over the cyt *bc*<sub>1</sub> complex. The  $g_x$ ,  $g_y$ , and  $g_z$  values are 1.786, 1.888, and 2.026 in the presence of stigmatellin and 1.770, 1.894, and 2.034 with myxothiazol. At several-fold higher concentrations of either inhibitor (not shown), no further changes of spectra were observed.

Spectra g and h in Figure 4 show similar measurements except that antimycin, the specific  $Q_1$  site inhibitor, was added. If the  $Q_0$  and  $Q_1$  sites are distinct and noninteracting (Robertson et al., 1986; Robertson & Dutton, 1988), then, in contrast to the findings with the  $Q_0$  site inhibitors, antimycin should have no effect on the [2Fe-2S] cluster. The similarity of the spectra a and b and spectra g and h demonstrates that this is the case.

These results confirm previous reports that unique interactions are introduced between the [2Fe-2S] cluster and either stigmatellin or myxothiazol bound to the  $Q_0$  site. More important, however, is the finding that the line shapes characteristic of the presence of myxothiazol or stigmatellin are observed when the inhibitor is added at or near stoichiometric equivalence with the cyt *bc*<sub>1</sub> complex (and, therefore, the  $Q_0$  site), independent of whether there are 26 or 2 Q per reaction

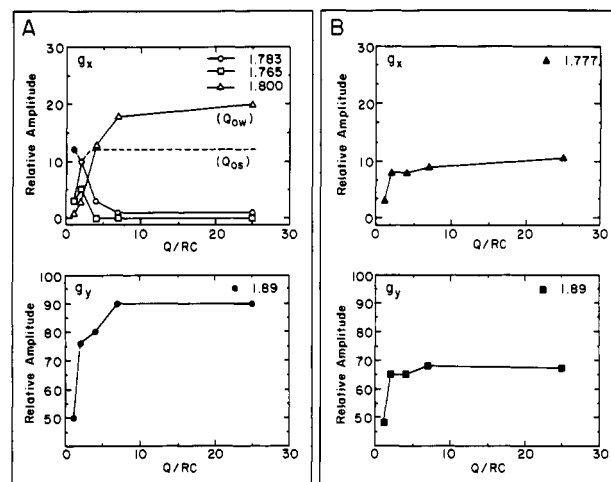


FIGURE 5:  $Q_0$  site occupancy by Q and  $QH_2$ . The data were taken from the EPR spectra in Figure 1. (Panel A) Signal amplitudes ( $g_x$  at 1.800 and 1.783) are presented as a function of the number of ubiquinones per reaction center remaining in chromatophores when  $Q_{\text{pool}}$  was oxidized. The amplitudes were measured at open arrows (shown in Figure 1A) in order to maximize resolution of the two bands for the analysis. The amplitude of the  $g_y$  band was measured directly from peak to peak. The dotted line represents the occupancy of the  $Q_{\text{os}}$  and will be referred to in Table I. (Panel B) Signal amplitudes ( $g_x$  at 1.777 and  $g_y$  at 1.890) are presented as a function of the number of ubiquinones per reaction center remaining in chromatophores when the  $Q_{\text{pool}}$  was reduced with sodium dithionite. The amplitude of  $g_x$  was measured from peak to baseline, obtained by drawing a straight line across the base of the signal. The  $g_y$  amplitude was measured from peak to peak (see Figure 1).

center present. This demonstrates that both the [2Fe-2S] cluster- $Q$  interactions giving rise to the  $g_x$  at 1.800 and 1.783 are eliminated by a single molecule of myxothiazol or stigmatellin in the  $Q_0$  site, suggesting that the same site probably mediates both interactions.

In experiments controlling for the effects on the [2Fe-2S] line shape of the solvents added with inhibitors described in the previous section, we found that a final concentration of 1% absolute ethanol (i.e., 170 mM) replaces the [2Fe-2S] line shape characteristic of  $Q$  presence in the  $Q_0$  site with a new [2Fe-2S] EPR line shape roughly similar to that of extensively extracted chromatophores shown previously in Figure 2, spectrum a. This appears to be a characteristic not shared with DMSO. The ethanol concentration that reduces the  $g_x$  at 1.800 to half amplitude is approximately 34 mM. Whether this means that ethanol displaces the ubiquinone or modifies the general environment of the [2Fe-2S] cluster cannot be decided from what we have done so far. However, the inhibitors, with their affinity for the  $Q_0$  site considerably higher than that of the native ubiquinone, are able to override the ethanol effect on a one molecule per site basis, indicating that the ethanol effect is reversible and specific to interactions with the [2Fe-2S] cluster emanating from the  $Q_0$  site.

#### Binding Affinities of the $Q_0$ site for Q and $QH_2$ Indicated by the Q and $QH_2$ Dependent Alterations in [2Fe-2S] Cluster EPR Spectra

Since the [2Fe-2S] line shape is significantly different when the ubiquinone is at physiological levels, partially extracted, or when nearly completely extracted, the binding affinities of the  $Q_0$  site for Q and  $QH_2$  can be determined using the EPR spectral line shapes as a measure of occupancy. The data shown in Figure 1, plotted as shown in Figure 5, were used to obtain the information.

Figure 5A shows a plot of the  $g_x$  amplitudes at 1.800 (representing the [2Fe-2S]- $Q_0$  site at physiological, high levels



of Q), at 1.783 (representing the [2Fe-2S]-Q<sub>o</sub> site after partial extraction and low levels of Q), and at 1.765 (representing the [2Fe-2S]-Q<sub>o</sub> site after exhaustive extraction and nearly free of Q). Contributions from each state were measured at magnetic field strengths at the minimum of the  $g_x$  at 1.800 position and at the high-field side of the 1.783 position to optimize resolution, as shown by the open arrows in Figure 1. In the case of the very weak signal at  $g_x$  at 1.765, the minimum was used, and some overlap with the  $g_x$  at 1.783 contribution was expected. Also plotted is the  $g_y$  at 1.890 peak-to-peak amplitude, unresolved for all the states.

Figure 5 shows the two Q-dependent transitions in the [2Fe-2S] cluster spectra that report the binding of Q to the Q<sub>o</sub> site. Between 7.0 and 2.2 Q per reaction center, there is a loss of the  $g_x$  at 1.800 form, a concomitant gain of the  $g_x$  at 1.783 form, and, consistent with the broader spectrum, a net 15–20% diminution of the  $g_y$  amplitude. Judging from the amplitude of the  $g_x$  at 1.800, which gives the clearest view of the course of the  $g_x$  at 1.800/1.783 transition, the half-point for the transition is about 4 Q per reaction center. The next step is seen between 2.2 and 1.1 Q per reaction center by the loss of the  $g_x$  at 1.783 and gain of the  $g_x$  at 1.765, and a further 25–30% diminution of the  $g_y$  amplitude, signaling that the Q<sub>o</sub> site is free of Q. The half-point of the  $g_x$  at 1.783/1.765 transition is in the range of 1–2 Q per reaction center.

Figure 5B describes the Q<sub>o</sub> site affinity for QH<sub>2</sub>. The data for the QH<sub>2</sub> binding profile are restricted because of the lack of a clear transition for QH<sub>2</sub> analogous to that seen for Q by the  $g_x$  at 1.800/1.783 transition and the loss of amplitude at  $g_y$ . The only indication for its existence is the small decrease in amplitude of  $g_x$  at 1.777 and  $g_y$  over the range of 7.0–2.2 QH<sub>2</sub> per reaction center. However, at lower QH<sub>2</sub> levels, it is clear, despite some overlap of the  $g_x$  at 1.777 with the  $g_x$  at 1.765 (Q<sub>o</sub> site free of QH<sub>2</sub>) and a smaller diminution of the amplitude at  $g_y$ , that the binding half-point for QH<sub>2</sub> is near the stoichiometric range of 1–2 molecules per reaction center.

There are two principal limitations of the measurements analyzed in Figure 5. First, we are not able to determine the affinity for QH<sub>2</sub> from transitions analogous to the  $g_x$  at 1.783/1.800 transition seen with Q. Second, the near stoichiometric binding of both Q and QH<sub>2</sub> as reflected by  $g_x$  at 1.783 or 1.777 precludes determining whether one is bound tighter than the other. These limitations are circumvented using an indirect approach described in the next section.

#### *Redox Titration of the [2Fe-2S] EPR Line Shape Giving the Relative Q<sub>o</sub> Site Binding Affinities for QH<sub>2</sub> and Q.*

Comparisons of the  $E_{m7}$  value of the Q/QH<sub>2</sub> couples in the Q<sub>o</sub> site with that in the Q<sub>pool</sub> can provide information on the relative binding affinities of the Q<sub>o</sub> site for QH<sub>2</sub> and Q. Combined with the  $E_{m7}$  value of the Q<sub>pool</sub>, a thermodynamic cycle permits the calculation of the relative affinity of the Q<sub>o</sub> site for Q and QH<sub>2</sub> according to

$$\log(K_{QH_2}/K_Q) = [E_{m7}(Q_{pool}) - E_{m7}(Q_o)]/30 \quad (1)$$

where  $K_Q$  and  $K_{QH_2}$  are the dissociation constants for Q and QH<sub>2</sub>, respectively.

$E_{m7}$  values for the resolved states of binding seen at high and low Q levels were obtained by measuring, as a function of redox potential, the amplitude of the  $g_x$  at 1.800 in native chromatophores or of the  $g_x$  at 1.783 in chromatophore preparations with approximately 2 ubiquinones per reaction center. Measurement of the  $g_x$  at 1.777 (the unresolved QH<sub>2</sub> occupancy) for each condition was also performed to improve the possibility of detecting complexities in the binding interactions. For instance, the simple expression described in eq

1 will apply only if there are no stable intermediate states. While we can be reasonably confident about the absence of stable semiquinone states associated with the Q<sub>o</sub> site at equilibrium under the conditions used (DeVries et al., 1986), the multiplicity of binding states, at least for Q, raises the possibility for greater complexity than accommodated by eq 1. Hence, we looked for deviations from simple Nernst behavior, as well as for indications of new EPR spectral forms of the [2Fe-2S] cluster.

Figure 6A shows sample spectra of the [2Fe-2S] cluster in the  $g_x$  region at different Q/QH<sub>2</sub> ratios established in chromatophores with a native sized Q<sub>pool</sub>. With the lowering of the redox potential and the decrease in the Q/QH<sub>2</sub> ratio, the prominent  $g_x$  at 1.800 diminishes concomitant with the appearance of the  $g_x$  at 1.777. Inspection of the spectra during the titration failed to reveal any clear new spectral contribution that would indicate the presence of stable intermediate states. At 81 mV, close to the midpoint of the transition (see below), spectrum c is matched, as shown in spectrum f, simply by half the sum of the spectra taken fully oxidized (spectrum a) and reduced (spectrum e). If intermediate states were indeed present, they were not detected under the present experimental conditions.

Figure 6B (top) shows the amplitudes of these  $g_x$  values as a function of redox potential. The  $g_x$  components of the states involved were sufficiently resolved to allow measurements at their respective peak positions. The data sets describe  $n = 2$  Nernst curves with an  $E_{m7}$  value at 80 mV for the loss of the  $g_x$  at 1.800 (the value from three determinations was  $80 \pm 5$  mV) and an  $E_{m7}$  value at 76 mV for the gain of the  $g_x$  at 1.777 (the value from three determinations was  $76 \pm 5$  mV). Additional corroborating data are shown in Figure 6B (bottom) for the expected drop of the  $g_y$  amplitude as the Q<sub>o</sub> site occupant changes from Q to QH<sub>2</sub>; in this case, again, a transition is seen with an  $E_{m7}$  value of  $81 \pm 5$  mV. These numbers, reflecting the  $E_{m7}$  value of the Q/QH<sub>2</sub> couple in the Q<sub>o</sub> site, are within experimental error of each other, which rules against the possibility that there are significant populations of stable intermediate redox forms during the titration. The values are also within experimental error of the  $E_{m7}$  value of the Q<sub>pool</sub>; an average value of all the EPR measurements on ubiquinone in the Q<sub>o</sub> site is 79 mV compared to 90 mV for the Q<sub>pool</sub>, indicating that the affinities of the Q<sub>o</sub> site for both Q and QH<sub>2</sub> are approximately equal. If the small difference was significant, it would indicate a less than 2.5-fold binding preference of the Q<sub>o</sub> site for Q over QH<sub>2</sub>.

Figure 6C,D shows similar measurements on chromatophores partially extracted to a ubiquinone level of 2.4 Q per reaction center to display the  $g_x$  at 1.783 spectrum. This is a more difficult measurement than described for the native Q<sub>pool</sub> above, because of the broader line shapes and their greater superposition. Nevertheless, the main features of the titration can be perceived. The  $n = 2$  Nernst curve through the points, showing the loss of  $g_x$  at 1.783 and gain at 1.777, has a midpoint at  $95 \pm 5$  mV, while for the  $g_y$  band diminution the midpoint is at  $98 \pm 5$  mV. Again, this suggests that the electrochemistry of the ubiquinone associated with the Q<sub>o</sub> site, characterized by the  $g_x$  at 1.783 when Q is present, is similar to that of the Q<sub>pool</sub>. Even if significant, the small positive shift in the midpoint of Q/QH<sub>2</sub> in the Q<sub>o</sub> site would represent a less than 2-fold preferential binding of the Q<sub>o</sub> site for QH<sub>2</sub> over Q.

Figure 6E describes controls for the titrations shown in panels A–D, done on chromatophores that, with the exception of the Q<sub>A</sub> site molecule, are nearly devoid of ubiquinone. As

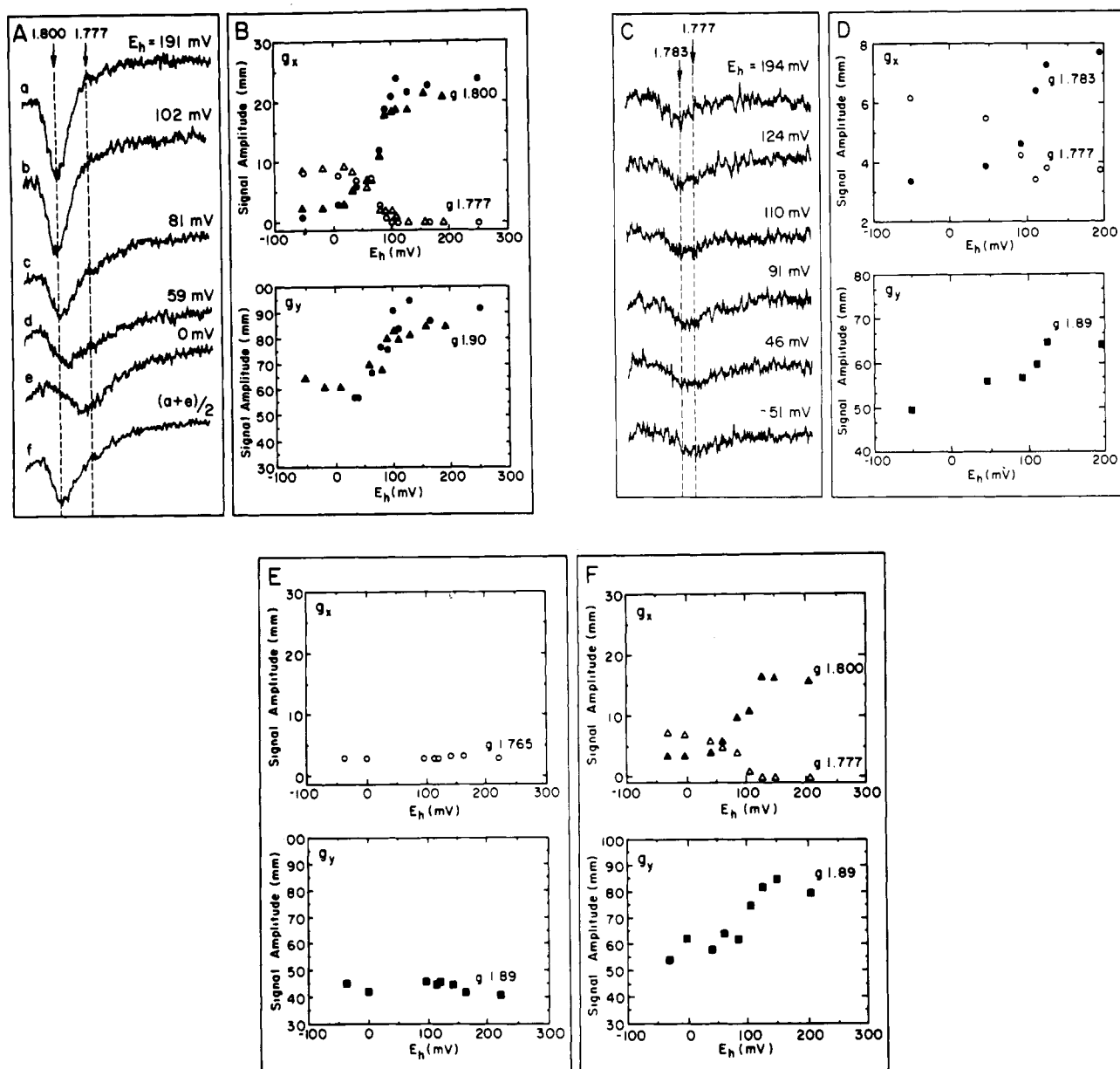


FIGURE 6: Redox titrations of the [2Fe-2S] cluster line-shape alteration in chromatophores at various  $Q_{\text{pool}}$  sizes. Chromatophores were suspended to 25  $\mu\text{M}$  reaction center in 50 mM MOPS and 100 mM KCl (pH 7.0). Panel A shows selected  $g_x$  transitions during the redox titration of [2Fe-2S] EPR spectra in native chromatophores containing 26 Q per reaction center. The redox potential is indicated on each spectrum. Spectrum f is half of the sum of spectrum a, which represents the  $Q_{\text{pool}}$  oxidized, and spectrum e, which represents the  $Q_{\text{pool}}$  reduced. Panel B shows the redox titration of the  $g_x$  amplitudes at 1.800, for Q occupancy, and at 1.777, for  $\text{QH}_2$  occupancy, and of the  $g_y$  in native chromatophores. The amplitude of the  $g_x$  band was measured from peak to baseline, obtained by drawing a straight line across the base of the signal. The  $g_y$  amplitude was measured from peak to peak. The symbols  $\Delta$  and  $\circ$  represent two different native chromatophore preparations containing 26 and 34 Q per reaction center, respectively. Panel C shows the  $g_x$  transition in partially extracted chromatophores containing 2.4 Q per reaction center during redox titration. Panel D shows the redox titration of the  $g_x$  amplitudes 1.783, for Q occupancy, and 1.777, for  $\text{QH}_2$  occupancy, and for the  $g_y$  peak to peak amplitudes in ubiquinone partially extracted chromatophores. Data were obtained from panel C. Panel E shows the redox titration of the  $g_x$  amplitude at 1.765 and the  $g_y$  peak to peak amplitude around 1.893 in extensively extracted chromatophores containing 1.0 Q per reaction center. Panel F shows a redox titration of the  $g_x$  amplitude at 1.800 and 1.777 and the  $g_y$  peak to peak amplitude around 1.890 in ubiquinone-10 reconstituted chromatophores (as shown in Figure 2, spectrum c). Redox mediators used in all these redox titrations were the same: 20  $\mu\text{M}$  each of 2,3,5,6-tetramethylphenylenediamine, *N*-methylphenazonium methosulfate, *N*-ethylphenazonium ethosulfate, and pyocyanine. The redox potential was adjusted through addition of freshly prepared, well-buffered solutions of sodium dithionite or potassium ferricyanide.

expected from Figure 1, spectrum e, the  $g_y$  at 1.893 and  $g_x$  at 1.765 amplitudes are independent of the ambient redox potential.

Figure 6F shows that the results of panels A and B can be recovered after reconstitution of extracted chromatophores with ubiquinone-10. Reconstitution of the material used in panel E, by addition of 40 Q per reaction center, yields spectra (not shown) and redox titrations that are essentially the same as for the unextracted native material. No attempt was made to reconstitute the titrations of panels C and D.

The redox titrations of Figure 6 show that the two Q-dependent spectral forms of the [2Fe-2S] cluster, reflecting a strongly bound Q (near stoichiometric) and a weaker bound Q (half-point 4Q/reaction center) to the  $Q_0$  site, each has a  $\text{QH}_2$  counterpart that binds to the site with similar affinity. We suggest that these affinities be used to define the strongly and weakly bound ubiquinones as  $Q_{\text{os}}$  and  $Q_{\text{ow}}$ , respectively. Thus, when the  $Q_{\text{os}}$  domain is occupied by Q, the [2Fe-2S] cluster is characterized by a  $g_x$  at 1.783, and, when both  $Q_{\text{os}}$  and  $Q_{\text{ow}}$  domains are occupied by Q, the  $g_x$  is at 1.800. The



Table I

		occupancy of cyt <i>bc</i> <sub>1</sub> sites [2Fe-2S] cluster transitions							
		occupancy of RC sites (Q/RC)		% max <i>g</i> <sub>x</sub> amplitude <sup>a</sup>		Q/RC <sup>b</sup>			
total Q per RC	Q <sub>A</sub> <sup>c</sup>	Q <sub>B</sub> <sup>c</sup>	1.783	1.800	Q <sub>os</sub>	Q <sub>ow</sub>	total Q assigned	total Q/RC unassigned	
1.1	0.85	0.10	25	0	0.15	0	1.1	0	
2.2	0.95	0.50	80	15	0.48	0.09	2.02	0.18	
4.1	1.00	0.85	100	65	0.60	0.40	2.85	1.25	
7.0	1.00	1.00	100	95	0.60	0.57	3.17	3.83	
25.0	1.00	1.00	100	100	0.60	0.60	3.2	21.8	

<sup>a</sup> The percent of the *g*<sub>x</sub> maximum amplitudes at 1.800 were obtained directly from the data of Figure 1. The percent of the *g*<sub>x</sub> maximum amplitude at 1.783 is not obtainable directly from Figure 1. This is because of the loss of amplitude of the *g*<sub>x</sub> at 1.783 at high Q/RC ratios due to the additional occupation of the Q<sub>ow</sub> domain. The maximum amplitude of the *g*<sub>x</sub> at 1.783 was obtained from its proposed inverse relationship with the amplitude at *g*<sub>x</sub> at 1.800 and, as shown by the dotted curve in Figure 5A, extrapolating to 1.1 Q/RC, ignoring the loss of Q binding to the Q<sub>os</sub> domain. The percent of maximum amplitude of the *g*<sub>x</sub> at 1.783 reporting the loss of Q binding to the Q<sub>os</sub> domain at 1.1 and 2.2 Q/RC relates to this amplitude as indicated by the closed circle at the end of dotted curve. At the higher Q/RC ratios, as the *g*<sub>x</sub> at 1.783 diminishes with the transition to 1.800, the Q<sub>os</sub> domain is assumed to remain occupied as indicated by the dashed line in Figure 5A. <sup>b</sup> The ratio of cyt *bc*<sub>1</sub> complex to reaction center is 0.6 in chromatophores (see Materials and Methods), thereby allowing the percent of the *g*<sub>x</sub> maximum amplitude to be converted into the number of Q molecules occupying the Q<sub>os</sub> and Q<sub>ow</sub> domains of the Q<sub>o</sub> site. <sup>c</sup> The occupancies of Q<sub>A</sub> and Q<sub>B</sub> in reaction center were measured kinetically in chromatophores at each extraction step as described under Materials and Methods.

analysis of Figure 1 suggests that, when Q<sub>os</sub> and Q<sub>ow</sub> are both occupied by QH<sub>2</sub>, the [2Fe-2S] cluster assumes very similar or identical spectra (both *g*<sub>x</sub> at 1.777). The *E*<sub>m7</sub> values for the QH<sub>2</sub>/Q couples in the Q<sub>os</sub> and Q<sub>ow</sub> domains are not significantly different from that of the Q<sub>pool</sub> value.

#### Comparison of the Q<sub>o</sub> Site Binding Affinities with Those of the Q<sub>A</sub> and Q<sub>B</sub> Sites

The first two columns of Table I list the occupancy of Q<sub>A</sub> and Q<sub>B</sub> sites in the ubiquinone-extracted chromatophores discussed above. As already mentioned, the Q<sub>A</sub> site is 85% occupied at 1.1 Q per reaction center, and, at this level of Q, only about 0.1 Q apparently occupies the Q<sub>B</sub> site. At 2.2 Q per reaction center, the Q<sub>A</sub> site is essentially fully occupied, while the Q<sub>B</sub> site approaches full apparent occupancy between 4.1 and 7.0 Q per reaction center.

In comparison, the Q<sub>o</sub> site occupancy shown by the loss of the *g*<sub>x</sub> at 1.765, gain at 1.783, and the enhancement of the *g*<sub>y</sub> amplitude (occupancy of the Q<sub>os</sub> domain by Q) is estimated to be 25% complete at 1.1 Q per reaction center and 80% complete at 2.2 Q per reaction center (Table I). The second Q-dependent transition that replaces *g*<sub>x</sub> at 1.783 with 1.800 (Q<sub>os</sub> and Q<sub>ow</sub> domains occupied by Q) is only 15% complete at 2.2 Q and, with the half-point at about 4 Q, achieves a maximum around 7.0 Q per reaction center.

If we make the reasonable assumption that each Q-dependent transition results from the binding of a single molecule to a single location in the cyt *bc*<sub>1</sub> complex, specifically the Q<sub>os</sub> and Q<sub>ow</sub> domains of the Q<sub>o</sub> site, and take into account that there were 0.6 cyt *bc*<sub>1</sub> complexes per reaction center in the chromatophores used in the measurements (i.e., 0.6 Q<sub>o</sub> sites accommodating one Q<sub>os</sub> and one Q<sub>ow</sub> domain per Q<sub>A</sub> site), these data can be presented on a molar basis. This allows some accounting, presented in the final columns of Table I, of the ubiquinones assigned to the Q<sub>A</sub> and Q<sub>B</sub> sites in the reaction center and the Q<sub>os</sub> and Q<sub>ow</sub> domains of the Q<sub>o</sub> site in the cyt *bc*<sub>1</sub> complex and, by difference, ubiquinones ascribable to the Q<sub>pool</sub> or as yet to be assigned to other sites.

#### DISCUSSION

**EPR Comparisons of the [2Fe-2S] Cluster of the Cyt *bc*<sub>1</sub> Complex of *R. capsulatus* with Others from Photosynthetic and Respiratory Systems.** The EPR *g* values of the different [2Fe-2S] cluster forms in the cyt *bc*<sub>1</sub> complex produced by various occupants in the Q<sub>o</sub> site reported in this work are

summarized in Table II, section A. If we examine previously published EPR spectra of [2Fe-2S] clusters when associated with intact cyt *bc*<sub>1</sub> complexes in a variety of native membranes [for example, DeVries et al. (1982a), Matsuura et al. (1983), and Robertson et al. (1984)], in detergent-isolated forms (Siedow et al., 1978; DeVries et al., 1979; Meinhardt et al., 1987; Yang & Trumpower, 1986; Andrews et al., 1989; McCurley et al., 1990; Berry et al., 1991), or when the [2Fe-2S] subunit is separated from the other cyt *bc*<sub>1</sub> complex subunits (Römissh et al., 1988; Hurt et al., 1981; DeVries, personal communication, and Link, Ohnishi, and von Jagow, unpublished data), we find that several of the spectral forms reported here for *R. capsulatus* are discernible. In some instances, these spectra are accompanied by other spectral forms [see DeVries (1986)], resulting, we suggest, from the following causes:

(a) Failure to establish the Q<sub>pool</sub> in a fully oxidized or reduced state by exposure to insufficiently high or low redox potentials or to disequilibrium between the poisoning redox couple and the Q<sub>pool</sub>.

(b) The multiplicity of components seen in cyt *bc*<sub>1</sub> complexes seems to become more evident when the associated Q<sub>pool</sub> is small. This is particularly the case for preparations isolated in detergent, which may be comprised of populations of cyt *bc*<sub>1</sub> complexes associated with Q trapped in the micelles at various levels. These conditions may produce a mixture of *g*<sub>x</sub> 1.765/1.783/1.800 line shapes. This may also apply to native mitochondrial membranes, since here the Q<sub>pool</sub> is much smaller (Kröger & Klingenberg, 1973) than it is in the photosynthetic bacteria. We also note that when solvent extraction has been used to remove the Q<sub>pool</sub>, the final molecule may not be extracted at all or may be only partially extracted, yielding a heterogeneous preparation.

(c) Use of ethanol as a solvent to make additions of reagents to the preparation can have a substantial effect on the [2Fe-2S] line shape, yielding much-broadened spectra. It is worth noting that 34 mM ethanol, which induces a roughly 50% loss of the *g*<sub>x</sub> at 1.800 amplitude when Q is present, is equivalent to the addition of only 2 μL of ethanol per milliliter of aqueous medium. Moreover, with few exceptions (Salerno & Ohnishi, 1976; DeVries et al., 1983), in published work on the [2Fe-2S] cluster of cyt *bc*<sub>1</sub> complexes, the nature of the solvent used in making additions of organic compounds is usually not recorded.

The best defined examples, for which there are suitable data representative of the different states of [2Fe-2S] clusters, are

Table II: *g* Values for Rieske-Type [2Fe-2S] Clusters

(A) Data from <i>R. capsulatus</i> with Different Components in the Q <sub>o</sub> Site					
	<i>g</i> <sub>av</sub>	<i>g</i> <sub>z</sub>	<i>g</i> <sub>y</sub>	<i>g</i> <sub>x</sub>	spectrum shown
X-[2Fe-2S]	1.893	2.026	1.893	1.765	Figure 1A, e
1 Q-[2Fe-2S]	1.898	2.023	1.890	1.783	Figure 1A, d
2 Q-[2Fe-2S]	1.903	2.019	1.890	1.800	Figure 1A, a
1 or 2 QH <sub>2</sub> -[2Fe-2S]	1.896	2.020	1.890	1.777	Figure 1B, a
1 stigmatellin-[2Fe-2S]	1.903	2.026	1.888	1.786	Figure 4, c and d
1 myxothiazol-[2Fe-2S]	1.902	2.034	1.894	1.770	Figure 4, e and f
mutant F144G	1.898	2.023	1.892	1.780	Figure 3, b
mutant F144L	1.894	2.024	1.894	1.765	Figure 3, c
(B) Some Selected Comparisons with [2Fe-2S] Clusters from Other Sources					
	<i>g</i> <sub>av</sub>	<i>g</i> <sub>z</sub>	<i>g</i> <sub>y</sub>	<i>g</i> <sub>x</sub>	reference
Isolated [2Fe-2S] Subunit					
green plant	0 Q <sup>a</sup>	2.02	1.89	?	Hurt et al. (1981) <sup>b</sup>
<i>N. crassa</i>	0 Q <sup>a</sup>	1.894	2.031	1.900	DeVries <sup>c</sup>
<i>N. crassa</i>	0 Q <sup>a</sup>	1.89	2.03	1.90	Römsisch et al. (1988)
beef heart	0 Q <sup>a</sup>	1.895	2.027	1.897	Link et al. <sup>d</sup>
[2Fe-2S] Cluster in Isolated Cyt <i>b<sub>6</sub>f</i> or Cyt <i>bc<sub>1</sub></i> Complex					
cyt <i>b<sub>6</sub>f</i> of plant		1.90	2.03	1.90	Riedel et al. (1991)
<i>R. capsulatus</i>	0.7 Q	1.891	2.019	1.893	Robertson <sup>e</sup>
<i>Rhodospirillum rubrum</i>	1.1 Q	1.90	2.02	1.90	Wynn et al. (1985)
		1.90	2.02	1.90	Güner et al. (1991)
<i>Paracoccus denitrificans</i>	3.5 Q	1.90	2.02	1.89	Yang et al. (1986)
	3.5 QH <sub>2</sub>	1.90	2.03	1.89	Yang et al. (1986)
<i>R. sphaeroides</i>	4.0 Q	1.91	2.03	1.90	Andrews et al. (1990)
<i>R. sphaeroides</i>	4.0 QH <sub>2</sub>	1.896	2.029	1.90	Andrews et al. (1990)
yeast	1.3 Q	1.908	2.025	1.89	Siedow et al. (1978)
yeast	1.3 QH <sub>2</sub>	1.902	2.026	1.89	Siedow et al. (1978)
Potato	0.2 Q	1.90	2.03	1.90	Berry et al. (1991) <sup>f</sup>
potato	0.2 QH <sub>2</sub>	1.90	2.03	1.90	Berry et al. (1991) <sup>f</sup>
beef heart	12.1 Q	1.905	2.019	1.891	DeVries et al. (1983)
beef heart	12.1 QH <sub>2</sub>	1.897	2.024	1.895	Devries et al. (1983)
[2Fe-2S] Cluster in Native Membrane					
chloroplast	PQ	?	2.01	1.90	Malkin (1982) <sup>b</sup>
beef heart	Q	1.905	2.020	1.894	DeVries et al. (1982a)
beef heart	QH <sub>2</sub>	1.897	2.019	1.890	DeVries et al. (1982a)
<i>R. sphaeroides</i>	Q	1.91	2.03	1.90	Matsuura et al. (1983)
<i>R. sphaeroides</i>	QH <sub>2</sub>	1.91	2.03	1.90	Matsuura et al. (1983)

<sup>a</sup>In isolated [2Fe-2S] subunit, we assume that no quinone was left in preparation. <sup>b</sup>No *g*<sub>x</sub> band is reported. <sup>c</sup>Personal communication; the [2Fe-2S] subunit was isolated from *N. crassa*. <sup>d</sup>Data from T. A. Link, T. Ohnishi, and G. von Jagow (unpublished). <sup>e</sup>The isolated cyt *bc*<sub>1</sub> complex from *R. capsulatus* contains 0.7 ubiquinone per *c*<sub>1</sub> (Robertson, unpublished). The [2Fe-2S] cluster was reduced with ascorbate. <sup>f</sup>The isolated cyt *bc*<sub>1</sub> complex from potato tuber mitochondria contains 0.15–0.25 ubiquinones per cyt *bc*<sub>1</sub> complex. The [2Fe-2S] EPR spectra are identical when the protein is reduced with hydroquinone or sodium dithionite.

included in Table II, section B. These generally are similar to the spectra of *R. capsulatus* under analogous conditions (section A of Table II) regardless of the biological source. Thus, the *g* values for the [2Fe-2S] clusters in the cyt *bc*<sub>1</sub> complex associated with native membranes with a full complement of ubiquinone are similar to the dominant spectral component of the [2Fe-2S] clusters in quinone-containing isolated cyt *bc*<sub>1</sub> complexes (Siedow et al., 1978; DeVries et al., 1979; Yang & Trumpower, 1986; Andrews et al., 1990). Also, the *g* values of the isolated [2Fe-2S] cluster subunit (Römsch et al., 1988; DeVries, personal communication, and Link, Ohnishi, and von Jagow, unpublished data) are similar to those of isolated preparations of cyt *bc*<sub>1</sub> complex with no or very low amounts of quinone present (Berry et al., 1991; Robertson et al., manuscript in preparation) or in solvent-extracted native membranes (see Figure 1, spectrum e, of this work). Past observations of the EPR spectra of the [2Fe-2S] clusters of the cyt *b*<sub>6</sub>f complex of chloroplast, with the exception of Salerno et al. (1983), had failed to show a discernible *g*<sub>x</sub> feature (Hurt et al., 1981; Malkin, 1982; Li et al., 1991). In fact, Riedel et al. (1991) have recently reported that the *g*<sub>x</sub> band in the cyt *b*<sub>6</sub>f [2Fe-2S] EPR spectrum could be detected at 1.76–1.74 under low microwave power but that it is not sensitive to the redox state of the plastoquinone in the membrane. These studies suggest that the interaction between Q in the Q<sub>o</sub> site and [2Fe-2S] cluster might be different between

the cyt *bc*<sub>1</sub> complex and cyt *b*<sub>6</sub>f complex.

**Biochemical Interpretations of the Interaction of Occupants of the Q<sub>o</sub> Site with the [2Fe-2S] Cluster.** The recent findings that the [2Fe-2S] clusters in phthalate dioxygenase from *Pseudomonas cepacia* (Cline et al., 1985), the "Rieske-type" [2Fe-2S] cluster of *Thermus thermophilus* (Fee et al., 1984), the cyt *bc*<sub>1</sub> complexes of *R. capsulatus* (Gurbiel et al., 1991), and several other organisms (Britt et al., 1991) are probably attached to the polypeptide via two histidines liganded to one of the Fe atoms (Gurbiel et al., 1989, 1991), provides an attractive possibility for hydrogen bonding from the imidazole NH to the carbonyl oxygen of Q and the phenoxyl of the QH<sub>2</sub> or other occupants of the Q<sub>o</sub> site (Keske et al., 1990). Similar arrangements have been proposed for the Q<sub>o</sub> site (Rich, 1989) and Q<sub>B</sub> site (Bunker et al., 1982; Wraight, 1982). In this arrangement, the [2Fe-2S] cluster acts both as an oxidant/reductant for ubiquinone and as a binding point for the occupant of the Q<sub>o</sub> site. Competition with ubiquinone for the imidazole hydrogen bond(s) could be one avenue for the action of inhibitors. A simple model, based on this dual functional character of the [2Fe-2S] cluster, has recently been presented (Robertson et al., 1990), although at that time only one histidine ligand on the [2Fe-2S] cluster was considered and only a single ubiquinone occupancy of the Q<sub>o</sub> site was proposed. The increasing evidence for the two histidines is timely in offering a simple way of explaining our evidence that the Q<sub>o</sub>

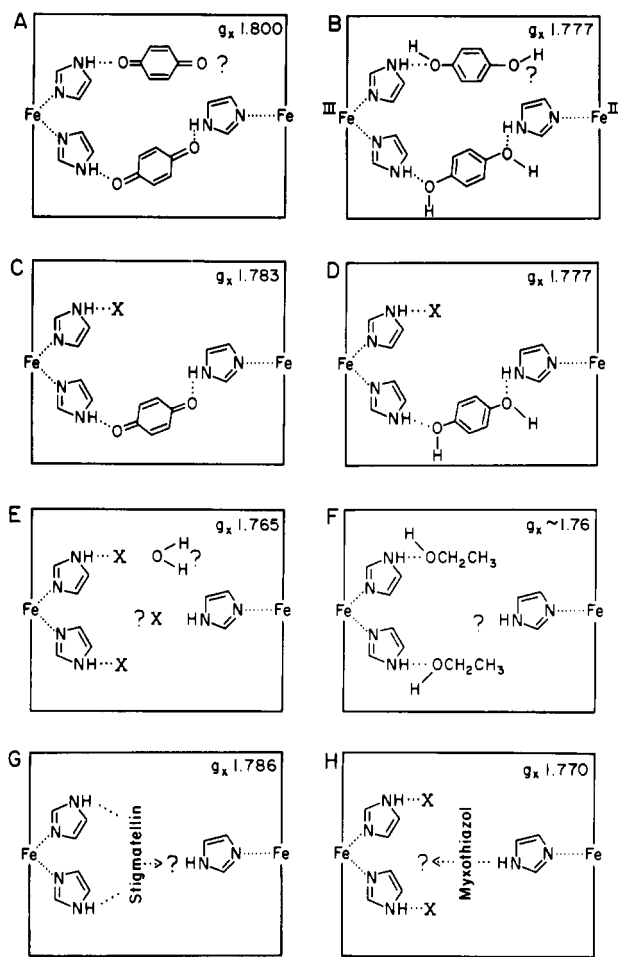


FIGURE 7: Summary of possible binding arrangements for various occupants of the  $Q_o$  site. See the text for details.

site can accommodate two ubiquinone molecules. Figure 7 schematically presents the extensions of our earlier single-occupancy model, focusing speculation on the two histidines of the  $[2Fe-2S]$  cluster and one of the axial ligands of cytochrome  $b_L$ . In the figure, one of the Q or  $QH_2$  is shown ligated to the histidines of the  $[2Fe-2S]$  and  $cyt\ b_L$  ( $Q_{os}$ ?), whereas the other is bound to the second histidine on the  $[2Fe-2S]$  cluster ( $Q_{ow}$ ?). Removal of the ubiquinones yields a new situation in which one or both is replaced by an unidentified ligand, X. Candidates for X are another hydrogen-bonding side chain, water, or both. Similarities in the line shapes of the  $[2Fe-2S]$  cluster in the 2X form and in the isolated polypeptide (see the  $g$  values in Table II) show that X can be provided by the  $[2Fe-2S]$  polypeptide or the solvent with no essential requirements from the cytochrome  $b$  polypeptide. The simplest interpretation probably is that X is water. The line shape, seen on addition of ethanol, suggests that X, in this case, may be the ethanol itself, although this effect could have its source elsewhere.

The observation that some  $Q_o$  inhibitors can raise the  $E_m$  of  $[2Fe-2S]$  was originally made by Bowyer et al. (1980) using UHDBT. Stigmatellin shifts the midpoint of the  $[2Fe-2S]$  from 290 mV to values higher than 540 mV in mitochondrial membranes (Von Jagow & Ohnishi, 1985); that is, it binds  $>10000$  times tighter when the  $[2Fe-2S]$  is reduced than when it is oxidized. For this reason, we show stigmatellin interacting directly with the  $[2Fe-2S]$  cluster, having displaced both of the ubiquinones. This latter suggestion is supported by the fact that the spectrum induced by the stigmatellin (one molar equivalent) is the same whether there are two or one Q (see

Figure 4) or even no Q (data not shown) in the  $Q_o$  site. Spectral alteration of the cytochrome  $b_L$  optical spectrum hints that stigmatellin may also interact with this cofactor (von Jagow & Ohnishi, 1985; Hauska et al., 1989), but conclusions on whether this interaction is direct or indirect cannot be made. A similar preference for binding when the  $[2Fe-2S]$  cluster is reduced suggests that UHNQ and UHDBT are in the same category as stigmatellin; characteristic  $[2Fe-2S]$  cluster line shapes are encountered for these inhibitors [see Matsuura et al. (1983) and McCurley et al. (1990)]. Also, the inhibitor HMHQQ is likely to be in this class (Zhu et al., 1982); its binding in mitochondrial preparations has been shown to depend on the redox state of the  $[2Fe-2S]$  cluster and to induce a distinct line shape.

Myxothiazol, on the other hand, has no electrochemical influences which might indicate major interactions with the  $[2Fe-2S]$  cluster. As with stigmatellin, myxothiazol does affect the spectrum of the reduced cytochrome  $b_L$  (von Jagow & Engle, 1981; Meinhardt & Crofts, 1982; Brandt et al., 1988). The somewhat weak evidence that this inhibitor interacts with the cytochrome  $b_L$  side of the site (as is shown in the figure) is supported by direct binding studies showing that myxothiazol binds to the  $cyt\ bc_1$  complex devoid of the  $[2Fe-2S]$  subunit (Brandt et al., 1988). However, the absence of electrochemical influences of myxothiazol on the  $[2Fe-2S]$  cluster does not rule out interactions with the  $[2Fe-2S]$  cluster. The possibility remains that the interaction strengths with the site, including the  $[2Fe-2S]$  cluster, are the same independent of the redox state of the  $[2Fe-2S]$  cluster. Moreover, the characteristic  $[2Fe-2S]$  cluster line shape induced by the presence of myxothiazol suggests some form of interaction with the cluster. Independent of this uncertainty, the finding that the  $[2Fe-2S]$  cluster line shape is the same in the presence of myxothiazol (one molar equivalent), when there are two, one, or no Q in the  $Q_o$  site, again favors the idea that no matter where it binds, its binding results in the exclusion of both ubiquinones. However, this idea contrasts with results reported by Brandt et al. (1988), in which they proposed that myxothiazol-type inhibitors do not replace the ubiquinone in the  $Q_o$  site.

The line shape of the  $[2Fe-2S]$  cluster indicates that single-site mutations in the  $cyt\ b$  polypeptide, such as those presented in Figure 3, can change the  $Q_o$  site from full to empty in native chromatophore membranes. This implies that, if the above interpretations are correct, the ubiquinone molecules in the  $Q_{os}$  and  $Q_{ow}$  binding domains must share sensitivities to alterations of some of the same residues. Thus, the F144L [Figure 3 and Robertson et al. (1990)] or G158D mutations (Robertson et al., 1984, 1990) cause virtually total loss of ubiquinone binding to both the  $Q_{os}$  and  $Q_{ow}$  binding domains, while F144G causes only the removal of one ubiquinone identifiable with the  $Q_{ow}$  domain. Single-site mutations in the  $[2Fe-2S]$  cluster polypeptide (Gatti et al., 1989) also can lead to EPR spectra that are reminiscent of a total loss of ubiquinone binding in the  $Q_o$  site. In this regard, it is worth pointing out that the common use of the  $g_y$  band to assay the concentration of the  $[2Fe-2S]$  polypeptide in mutant membranes will, in the event of loss of Q from the  $Q_o$  site, lead to an underestimate by 40% because of the line-shape broadening described above (Figure 1).

**Redox Potentials of the  $Q_o$  Site Ubiquinones.** The  $E_m$  values for ubiquinone in the  $Q_o$  site have been derived previously from kinetic analyses of  $QH_2$ -mediated reduction of flash-oxidized  $cyts\ c_2$  and  $c_1$  (via the  $Q_o$  site and the  $[2Fe-2S]$  cluster) in chromatophores (Dutton & Jackson, 1972; Cogdell et al., 1972; Crofts et al., 1977; Matsuura et al., 1981; Prince

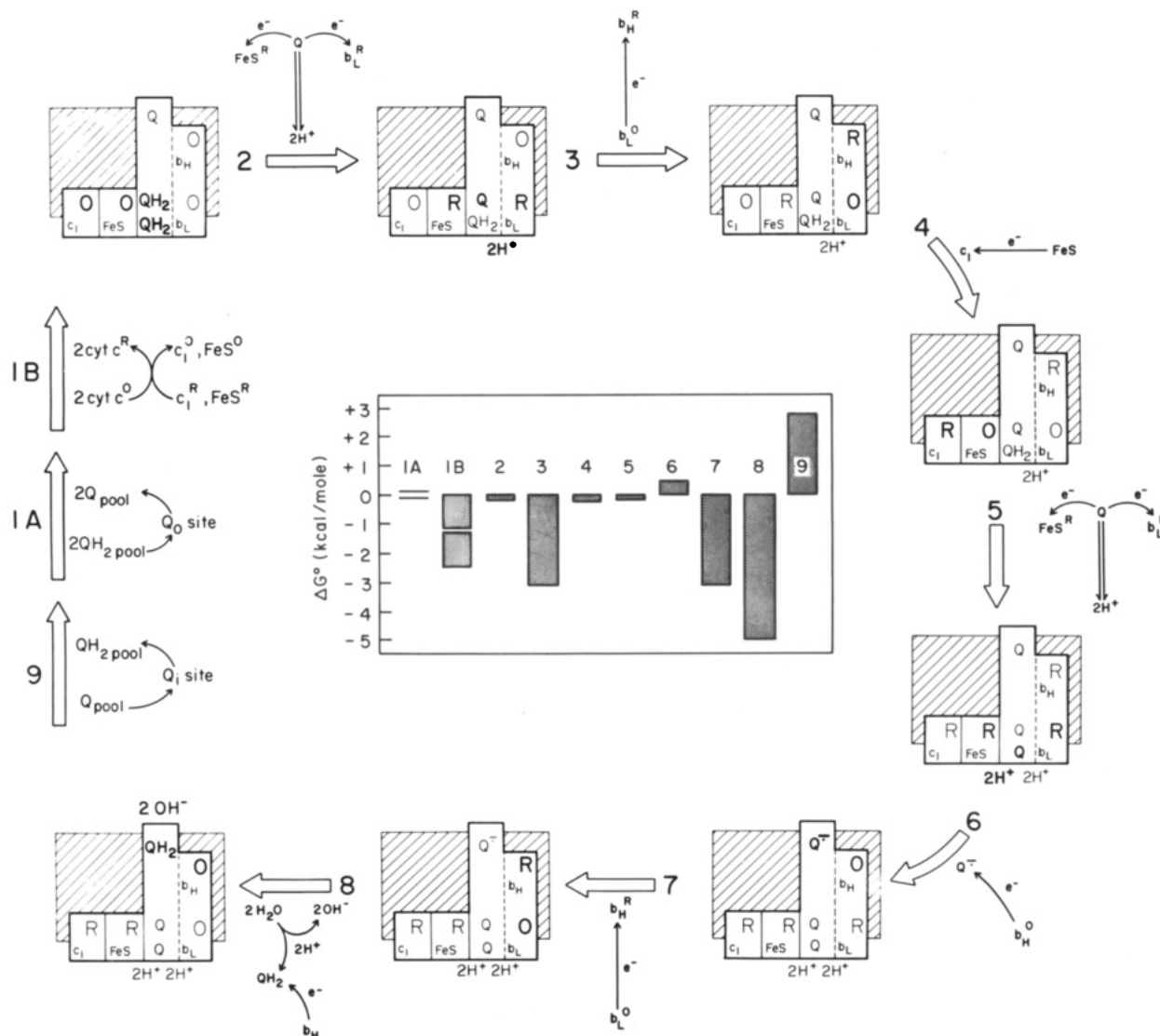


FIGURE 8: Double-occupancy  $Q_0$  site model for  $cyt\ bc_1$  complex turnover. The individual steps, shown for the operation of a complete turnover of the  $cyt\ bc_1$  complex, are arranged roughly in accordance with the time course of the reaction sequence but are artificially resolved in time for reasons of clarity. In any pair of diagrams depicting a particular step in the sequence, the cofactors that undergo a redox change are indicated by bold characters. Above each open arrow, pointing in the net physiological direction of the sequence, there is a thumbnail sketch that indicates the nature of the reaction. The lightly hatched background represents the membrane. The group of boxes represents the three subunits,  $cyt\ c_1$ , the [2Fe-2S] cluster, and  $cyt\ b$ ; the dashed line in the latter separates the  $Q_i$  and  $Q_o$  sites from the hemes. The locations of the cofactors in the profile of the membrane come from functional and indirect structural studies (Rich, 1984; Glaser & Crofts, 1984; Dutton, 1986; Konstantinov & Popova, 1988; Robertson & Dutton, 1988). The center of the figure graphically presents the standard free energies (pH 7.0) for each step, calculated from the  $E_{m7}$  values of the redox cofactors. The  $E_{m7}$  values are as follows:  $cyt\ c_2$ , 350 mV (Prince & Dutton, 1977);  $cyt\ c_1$ , 290 mV (D. E. Robertson, unpublished results); 2Fe2S cluster, 288 mV [average of Robertson et al. (1986) (270 mV), Prince et al. (1975) (310 mV), and D. E. Robertson, unpublished results (285 mV)];  $Q_{pool}$ , 90 mV (this work);  $Q_{os}$ , 87 mV;  $Q_{ow}$ , 87 mV (this work; the  $Q_{os}$  and  $Q_{ow}$  determined  $E_{m7}$  values of 95 and 79 mV have been averaged, since the quality of redox titrations does not justify making a distinction between the  $E_{m7}$  values of the  $QH_2/Q$  couples in the  $Q_{os}$  and  $Q_{ow}$  domains of the  $Q_0$  site). The data for  $cyt\ b_L$ , -90 mV (Petty & Dutton, 1976; Meinhardt & Crofts, 1983);  $cyt\ b_H$ , 50 mV (Petty & Dutton, 1976; Meinhardt & Crofts, 1983);  $Q_i$  ( $Q_i^-/Q_i$ ), 30 mV; and  $Q_i$  ( $Q_iH_2/Q_i^-$ ), 270 mV (Robertson et al., 1984) are from *R. sphaeroides*. (Reaction 1A) Exchange of Q for  $QH_2$  in each of the  $Q_{os}$  and  $Q_{ow}$  domains is presented as one reaction, for brevity. Since Q and  $QH_2$  bind nearly equally in each domain, the total  $\Delta G^\circ$  for the exchange of two Q for two  $QH_2$  is close to zero. (Reaction 1B) Oxidation of  $cyt\ c_1$  and the [2Fe-2S] cluster by two ferri- $cyt\ c_2$  is presented as one reaction, for brevity. (Reaction 2) The first  $QH_2$  oxidized through the cooperative action of the [2Fe-2S] cluster and the  $cyt\ b_L$ . At present, it is not known whether the  $Q_{os}$  or  $Q_{ow}$  is oxidized first, but, since the two have a similar  $E_{m7}$  value, this does not affect the overall  $\Delta G^\circ$  of the reaction. (Reaction 3) The  $\Delta G^\circ$  of electron transfer from the reduced  $cyt\ b_L$  to the oxidized  $cyt\ b_H$  is calculated assuming that there is no coupling of this reaction to the generation of membrane potential; i.e., it is "uncoupled". If coupled, the apparent  $\Delta G^\circ$  value will be less negative. The  $E_{m7}$  value for the  $cyt\ b_H$  is 50 mV, but, since we assume that no protons are obligatorily coupled to the reduction of the heme, we have taken the value of 20 mV, found above the pK value of the reduced form (Petty & Dutton, 1976). If protons are coupled to the reaction, the energetics do not change markedly. (Reaction 4) This is the reoxidation by  $cyt\ c_1$  of the reduced [2Fe-2S] cluster. (Reaction 5) This is a repeat of reaction 2. (Reaction 6) This endergonic electron transfer from the reduced  $cyt\ b_H$  to  $Q_i$  is presented as not being coupled to proton binding, in accordance with the established pKs of the product semiquinone anion in *R. sphaeroides* and mitochondria (Robertson et al., 1984). Current evidence supports a similar conclusion for *R. capsulatus* (Robertson & Dutton, 1988). (Reaction 7) This is a repeat of reaction 3. (Reaction 8) Electron transfer from the reduced  $cyt\ b_H$  to the  $Q_i$  semiquinone is presented coupled to the binding of two protons in accordance with the properties of the  $Q_i^-/QH_2$  reaction (Robertson et al., 1984). The  $E_{m7}$  value of 150 mV for the  $Q/QH_2$  in the  $Q_i$  site, taken together with the relatively low stability of the semiquinone at pH 7.0, makes this the most exergonic reaction of the sequence. (Reaction 9) The exchange, for Q, of the  $QH_2$  formed in reaction 8 in the  $Q_i$  site is endergonic. This is the price paid for the aid to the electron-transfer reaction in reaction 6 provided by the  $E_{m7}$  value of 150 mV for the  $Q/QH_2$  in the  $Q_i$  site. The 60-mV difference between the  $E_{m7}$  values of the  $Q/QH_2$  in the  $Q_i$  site and the  $Q_{pool}$  means that  $QH_2$  binds 100-fold tighter (2.72 kcal/mol) than Q.

et al., 1978; Crofts & Wang, 1989; Robertson et al., 1990). However, the point has been made by Crofts et al. (1977) and later by Bashford et al. (1979) that the kinetic approach for the determination of the  $E_m$  values for the  $Q_o$  site ubiquinone is vulnerable to misinterpretation, because the measurements are influenced by the rates of a variety of peripheral reactions that include  $QH_2/Q$  binding/release, lifetimes of the activated oxidizing state, and the overall catalytic rate. In showing that the  $E_{m7}$  values of ubiquinones in both the  $Q_{os}$  and  $Q_{ow}$  domains are similar to that of the  $Q_{pool}$  and not that indicated by kinetic assay [113 mV (Robertson et al., 1990); 130 mV (Evans & Crofts, 1974)], the present work with *R. capsulatus* appears to substantiate this point. Moreover, in earlier studies with *R. sphaeroides*, the  $E_{m7}$  value of the  $Q_o$  site quinones indicated by the [2Fe-2S] line-shape change (i.e., between  $g_x$  at 1.81 and 1.79 in the presence of a native  $Q_{pool}$ ) is also the same as that of the  $Q_{pool}$  (90 mV) (Matsuura et al., 1983) and not that obtained kinetically [155 mV; see Prince et al. (1978)].

**A Functional Double-Occupancy  $Q_o$  Site Model for the Cyt  $bc_1$  Complex.** The work presented above allows us to extend current models of the cyt  $bc_1$  complex in its functional role as a ubihydroquinone-cytochrome  $c$  oxidoreductase. The main pieces of new information are 2-fold:

(a) The  $Q_o$  site has two binding domains designated  $Q_{os}$  and  $Q_{ow}$ , which have a strong and weak interaction with ubiquinone. Although, at this stage, the reason for strong and weak binding interactions can only be guessed at, the affinities of both are in the range described by the reaction center  $Q_A$  and  $Q_B$  sites, and both interactions seem likely to play functional roles. Indeed, the existence of two binding sites for ubiquinone could allow the cyt  $bc_1$  complex to complete a full turnover without exchanging ubiquinone molecules with the pool. This mechanistic device contrasts with the current widely accepted models in which the oxidations of the two  $QH_2$  molecules required for the full enzymatic turnover occur at a single location in the  $Q_o$  site and proceed as two serial cycles of binding ( $QH_2$ ), oxidation, and release ( $Q$ ). This in-series mechanism is most explicit, for example, in the "double Q-cycle" version of the Q-cycle (Crofts & Wraight, 1983; Crofts & Wang, 1989).

Figure 8 presents a model that incorporates the  $Q_{os}$  and  $Q_{ow}$  binding domains of the  $Q_o$  site. It includes the ubiquinone binding reactions at the  $Q_o$  and  $Q_i$  sites, the electron transfer and protolytic reactions that catalyze the net oxidation of one  $QH_2$  to  $Q$ , and the reduction of two molecules of ferri-cyt  $c_2$  to ferro-cyt  $c_2$ .

(b) Knowledge of the  $E_{m7}$  values of the ubiquinones of the  $Q_{os}$  and  $Q_{ow}$  binding domains of the  $Q_o$  site furnishes information required to describe the standard free energies for the principal steps of the catalytic cycle. The center of Figure 8 shows the standard free energies of each of these steps in a way similar to that done for cytochrome  $c$  oxidase (Wikström & Babcock, 1990); the legend contains the basic information required for the calculations, which is derived from redox properties of the components of *R. capsulatus* or *R. sphaeroides*.

While the model shown in Figure 8 does not provide a unique solution to our results, it is perhaps the most parsimonious. Currently, however, our double-occupancy  $Q_o$  site model does not rule out the additional involvement of super-complexes (Joliet et al., 1989). Over a decade ago, DeVries, Slater, and co-workers (DeVries et al., 1979, 1982a) proposed an imaginative, more elaborate model for cytochrome  $bc_1$  complex function on the basis of the broad and narrow [2Fe-2S] cluster line shapes, which they attributed to the two

partners in a heterodimer of the cytochrome  $bc_1$  complex. Evidence preventing a ready interpretation of the resolved states of the [2Fe-2S] cluster of our work (e.g.,  $g_x$  at 1.800 and 1.783) as parts of such a dimeric model is the finding, most clearly presented in Figures 1 and 5, that the states are not seen independently, but are dependent upon the  $Q$  concentration and are mutually exclusive. This situation would not be expected in a heterodimer with each monomer having a separated, single-occupancy  $Q_o$  site and a characteristic line shape but could be included in a dimeric model in which there are close interactions between the single-occupancy  $Q_o$  sites and [2Fe-2S] clusters of the monomeric partners.

#### ACKNOWLEDGMENTS

We are very grateful to Dr. Simon DeVries for recalculating the  $g$  values for the isolated [2Fe-2S] cluster polypeptide from *Neurospora crassa* and for the valuable information provided in several discussions. We thank Drs. Link, Ohnishi, and von Jagow for providing us the unpublished  $g$  values of isolated [2Fe-2S] subunit.

#### REFERENCES

- Andrews, K. M., Crofts, A. R., & Gennis, R. B. (1990) *Biochemistry* 29, 2645-2651.
- Atta-Asafo-Adjei, E., & Daldal, F. (1991) *Proc. Natl. Acad. Sci. U.S.A.* 88, 492-496.
- Baccarini-Melandri, A., Gabellini, N., & Melandri, B. A. (1982) in *Functions of Quinones in Energy Conserving Systems* (Trumpower, B. L., Ed.) pp 258-298, Academic Press, New York.
- Barr, R., & Crane, F. L. (1971) *Methods Enzymol.* 23, 372-408.
- Bashford, C. L., Prince, R. C., Takamiya, K., & Dutton, P. L. (1979) *Biochim. Biophys. Acta* 545, 223-235.
- Berry, E. A., Huang, L.-S., & DeRose, V. J. (1991) *J. Biol. Chem.* 266, 9065-9077.
- Bevington, P. R. (1969) in *Data Reduction and Error Analysis for the Physical Sciences*, pp 204-246, McGraw-Hill, New York.
- Bowyer, J. R., Dutton, P. L., Prince, R. C., & Crofts, A. R. (1980) *Biochim. Biophys. Acta* 592, 445-460.
- Brandt, U., Schagger, H., & von Jagow, G. (1988) *Eur. J. Biochem.* 173, 499-506.
- Britt, R. D., Sauer, K., Klein, M. P., Knaff, D. B., Krauciunas, A., Yu, C.-A., Yu, L., & Malkin, R. (1991) *Biochemistry* 30, 1892-1901.
- Bunker, G., Stern, E. A., Blankenship, R. E., & Parson, W. W. (1982) *Biophys. J.* 37, 539-551.
- Clayton, R. K. (1963) in *Bacterial Photosynthesis* (Gest, H., San Pietro, A., & Veron, L. P., Eds.) p 498, Antioch Press, Yellow Springs, OH.
- Cline, J. F., Hoffman, B. M., Mims, W. B., LaHaie, E., Ballou, D. P., & Fee, J. A. (1985) *J. Biol. Chem.* 260, 3251-3254.
- Cogdell, R. J., Jackson, J. B., & Crofts, A. R. (1972) *J. Bioenerg.* 4, 413-429.
- Cramer, W. A., & Knaff, D. B. (1989) in *Energy Transduction in Biological Membranes*, Springer-Verlag, New York.
- Crofts, A. R., & Wraight, C. A. (1983) *Biochim. Biophys. Acta* 726, 149-185.
- Crofts, A. R., & Wang, Z. (1989) *Photosynth. Res.* 22, 69-87.
- Crofts, A. R., Crowther, D., Bowyer, J., & Tierney, G. V. (1977) in *Structure and Function of Energy Transducing Membranes* (van Dam, K., & van Gelder, B. F., Eds.) pp 133-155, Elsevier/North, Amsterdam, Holland.

- Crofts, A. R., Meinhardt, S. W., Jones, K. R., & Snozzi, M. (1983) *Biochim. Biophys. Acta* 723, 202–218.
- DeVries, S. (1986) *J. Bioenerg. Biomembr.* 18, 195–224.
- DeVries, S., Albracht, S. P. J., & Leuwerik, F. J. (1979) *Biochim. Biophys. Acta* 546, 316–333.
- DeVries, S., Albracht, S. P. J., Berden, J. A., & Slater, E. C. (1982a) *Biochim. Biophys. Acta* 681, 41–53.
- DeVries, S., Berden, J. A., & Slater, E. C. (1982b) in *Function of Quinones in Energy Conserving Systems* (Trumpower, B. L., Ed.) pp 235–246, Academic Press, New York.
- DeVries, S., Albracht, S. P. J., Berden, J. A., Marres, C. A. M., & Slater, E. C. (1983) *Biochim. Biophys. Acta* 723, 91–103.
- Dutton, P. L. (1978) *Methods Enzymol.* 54, 411–435.
- Dutton, P. L. (1986) in *Encyclopedia of Plant Physiology* (Staelin, A., & Arntzen, C. J., Eds.) Vol. 19, pp 197–237, Springer Verlag, West Berlin.
- Dutton, P. L., & Jackson, J. B. (1972) *Eur. J. Biochem.* 30, 495–510.
- Dutton, P. L., Petty, K. M., Bonner, H. S., & Morse, S. D. (1975) *Biochim. Biophys. Acta* 387, 536–556.
- Evans, E. H., & Crofts, A. R. (1974) *Biochim. Biophys. Acta* 357, 89–102.
- Fee, J. A., Finding, K. L., Yoshida, T., Hille, R., Tarr, G. E., Hearshen, D. O., Dunham, W. R., Day, E. P., Kent, T. A., & Münck, E. (1984) *J. Biol. Chem.* 259, 124–133.
- Gatti, D. L., Meinhardt, S. W., Ohnishi, T., & Tzagoloff, A. (1989) *J. Mol. Biol.* 205, 421–435.
- Glaser, E. G., & Crofts, A. R. (1984) *Biochim. Biophys. Acta* 766, 322–333.
- Güner, S., Robertson, D. E., Yu, L., Qiu, Z., Yu, C. A., & Knaff, D. B. (1991) *Biochim. Biophys. Acta* 1058, 269–279.
- Gurbiel, R. J., Batie, C. J., Sivaraja, M., True, A. E., Fee, J. A., Hoffman, B. M., & Ballou, D. P. (1989) *Biochemistry* 28, 4861–4871.
- Gurbiel, R. J., Ohnishi, T., Robertson, D. E., Daldal, F., & Hoffman, B. M. (1991) *Biochemistry* 30, 11579–11584.
- Hagen, W. R., Hearshen, D. O., Harding, L. J., & Dunham, W. R. (1985) *J. Magn. Reson.* 61, 233–244.
- Hauska, G., Herold, E., Huber, C., Nitschke, W., & Sofrova, D. (1989) *Z. Naturforsch., C: Biosci.* 44, 462–467.
- Hurt, H., Hauska, G., & Malkin, R. (1981) *FEBS Lett.* 134, 1–5.
- Jackson, J. B. (1988) in *Bacterial Energy Transduction* (Anthony, C., Ed.) pp 317–376, Academic Press, London.
- Joliot, P., Vermeglio, A., & Joliot, A. (1989) *Biochim. Biophys. Acta* 975, 336–345.
- Keske, J. M., Bruce, J. M., & Dutton, P. L. (1990) *Z. Naturforsch. C: Biosci.* 45, 430–435.
- Konstantinov, A. A., & Popova, E. (1988) in *Cytochrome Systems: Molecular Biology and Bioenergetics* (Papa, S., Chance, B., & Ernster, L., Eds.) pp 751–765, Plenum Press, New York.
- Kröger, A., & Klingenberg, M. (1973) *Eur. J. Biochem.* 34, 358–368.
- Li, L.-B., Zou, Y.-B., Yu, L., & Yu, C.-A. (1991) *Biochim. Biophys. Acta* 1057, 215–222.
- Malkin, R. (1982) *Biochemistry* 21, 2945–2950.
- Matsuura, K., Packham, N. Y., Mueller, P., & Dutton, P. L. (1981) *FEBS Lett.* 131, 17–22.
- Matsuura, K., Bowyer, J. R., Ohnishi, T., & Dutton, P. L. (1983) *J. Biol. Chem.* 258, 1571–1579.
- McCurley, J. P., Miki, T., Yu, L., & Yu, C.-A. (1990) *Biochim. Biophys. Acta* 1020, 176–186.
- Meinhardt, S. W., & Crofts, A. R. (1982) *FEBS Lett.* 149, 217–222.
- Meinhardt, S. W., & Crofts, A. R. (1983) *Biochim. Biophys. Acta* 723, 219–230.
- Meinhardt, S. W., Yang, X., Trumpower, B. L., & Ohnishi, T. (1987) *J. Biol. Chem.* 262, 8702–8706.
- Mitchell, P. (1975) *FEBS Lett.* 56, 1–6.
- Mitchell, P. (1976) *J. Theor. Biol.* 62, 327–367.
- Ohnishi, T., & Trumpower, B. L. (1980) *J. Biol. Chem.* 255, 3278–3284.
- Ohnishi, T., Brandt, U., & von Jagow, G. (1988) *Eur. J. Biochem.* 176, 385–389.
- Okamura, M. Y., Isaacson, R. H., & Feher, G. (1975) *Proc. Natl. Acad. Sci. U.S.A.* 72, 3491–3495.
- Petty, K. M., & Dutton, P. L. (1976) *Arch. Biochem. Biophys.* 172, 335–345.
- Prince, R. C. (1990) in *The Bacteria*, Vol. 12, pp 111–149, Academic Press, New York and London.
- Prince, R. C., & Dutton, P. L. (1977) *Biochim. Biophys. Acta* 459, 573–577.
- Prince, R. C., Lindsay, J. G., & Dutton, P. L. (1975) *FEBS Lett.* 51, 108–111.
- Prince, R. C., Bashford, L. C., Takamiya, K.-I., van den Berg, W. H., & Dutton, P. L. (1978) *J. Biol. Chem.* 253, 4137–4142.
- Rich, P. R. (1984) *Biochim. Biophys. Acta* 768, 53–79.
- Rich, P. R. (1989) in *Highlights of Modern Biochemistry* (Kotyk, A., et al., Eds.) Vol. I, pp 903–912, VSP Publishers, Prague.
- Riedel, A., Rutherford, A., Hauska, G., Müller, A., & Nitschke, W. (1991) *J. Biol. Chem.* 266, 17838–17844.
- Robertson, D. E., & Dutton, P. L. (1988) *Biochim. Biophys. Acta* 935, 273–291.
- Robertson, D. E., Prince, R. C., Bowyer, J. R., Matsuura, K., Dutton, P. L., & Ohnishi, T. (1984) *J. Biol. Chem.* 259, 1758–1763.
- Robertson, D. E., Davidson, E., Prince, R. C., van den Berg, W. H., Marrs, B. L., & Dutton, P. L. (1986) *J. Biol. Chem.* 261, 584–591.
- Robertson, D. E., Daldal, F., & Dutton, P. L. (1990) *Biochemistry* 29, 11249–11260.
- Römisch, J., Harnish, U., Schulte, U., & Weiss, H. (1988) in *Cytochrome Systems: Molecular Biology and Bioenergetics* (Papa, S., Chance, B., & Ernster, L., Eds.) pp 303–308, Plenum Press, New York.
- Salerno, J. C., & Ohnishi, T. (1976) *Arch. Biochem. Biophys.* 176, 757–765.
- Salerno, J. C., McGill, J. W., & Gerstle, G. C. (1983) *FEBS Lett.* 162, 257–261.
- Salerno, J. C., Osgood, M., Liu, Y., Taylor, H., & Scholes, C. P. (1990) *Biochemistry* 29, 6987–6993.
- Siedow, J. N., Power, S., de la Rosa, F. F., & Palmer, G. (1978) *J. Biol. Chem.* 253, 2392–2399.
- Takamiya, K.-I., & Dutton, P. L. (1979) *Biochim. Biophys. Acta* 546, 1–16.
- Takamiya, K.-I., Prince, R. C., & Dutton, P. L. (1979b) *J. Biol. Chem.* 254, 11307–11311.
- Urban, P. F., & Klingenberg, M. (1969) *Eur. J. Biochem.* 9, 519–525.
- van den Berg, W. H., Prince, R. C., Bashford, C. L., Takamiya, K., Bonner, W. D., & Dutton, P. L. (1979) *J. Biol. Chem.* 254, 8594–8604.
- Venturoli, G., Fernandez-Velasco, J. G., Crofts, A. R., & Melandri, B. A. (1986) *Biochim. Biophys. Acta* 851, 340–352.



- Vermeglio, A., & Clayton, R. K. (1977) *Biochim. Biophys. Acta* 461, 159–165.
- Von Jagow, G., & Engle, W. D. (1981) *FEBS Lett.* 136, 19–24.
- Von Jagow, G., & Ohnishi, T. (1985) *FEBS Lett.* 185, 311–315.
- Von Jagow, G., & Link, T. A. (1986) *Methods Enzymol.* 126, 253–271.
- Wikström, M., & Babcock, G. T. (1990) *Nature* 348, 16–17.
- Wraight, C. A. (1979) *Biochim. Biophys. Acta* 548, 309–327.
- Wraight, C. A. (1982) in *Function of Quinones in Energy Conserving Systems* (Trumpower, B. L., Ed.) pp 181–197, Academic Press, New York.
- Wynn, R. M., Gaul, D. F., Shaw, R. W., & Knaff, D. B. (1985) *Arch. Biochem. Biophys.* 238, 373–377.
- Yang, X., & Trumpower, B. L. (1986) *J. Biol. Chem.* 261, 12282–12289.
- Zhu, Q. S., Berden, J. A., DeVries, S., Folkers, K., Porter, T., & Slater, E. C. (1982) *Biochim. Biophys. Acta* 682, 160–167.

## Acetylene Inhibition of *Azotobacter vinelandii* Hydrogenase: Acetylene Binds Tightly to the Large Subunit<sup>†</sup>

Jin-Hua Sun, Michael R. Hyman, and Daniel J. Arp\*

Laboratory for Nitrogen Fixation Research, Oregon State University, 2082 Cordley Hall, Corvallis, Oregon 97331-2902

Received October 18, 1991; Revised Manuscript Received January 6, 1992

**ABSTRACT:** Acetylene is a slow-binding inhibitor of the Ni- and Fe-containing dimeric hydrogenase isolated from *Azotobacter vinelandii*. Acetylene was released from hydrogenase during the recovery from inhibition. This indicates that no transformation of acetylene to another compound occurred as a result of the interaction with hydrogenase. However, the release of C<sub>2</sub>H<sub>2</sub> proceeds more rapidly than the recovery of activity, which indicates that release of C<sub>2</sub>H<sub>2</sub> is not sufficient for recovery of activity. Acetylene binds tightly to native hydrogenase; hydrogenase and radioactivity coelute from a gel permeation column following inhibition with <sup>14</sup>C<sub>2</sub>H<sub>2</sub>. Acetylene, or a derivative, remains bound to the large 65 000 MW subunit (and not to the small 35 000 MW subunit) of hydrogenase following denaturation as evidenced by SDS-PAGE and fluorography of <sup>14</sup>C<sub>2</sub>H<sub>2</sub>-inhibited hydrogenase. This result suggests that C<sub>2</sub>H<sub>2</sub>, and by analogy H<sub>2</sub>, binds to and is activated by the large subunit of this dimeric hydrogenase. Radioactivity is lost from <sup>14</sup>C<sub>2</sub>H<sub>2</sub>-inhibited protein during recovery. The inhibition is remarkably specific for C<sub>2</sub>H<sub>2</sub>: propyne, butyne, and ethylene are not inhibitors.

The nitrogen-fixing bacterium *Azotobacter vinelandii* expresses a single, membrane-bound hydrogenase. The physiological function of this enzyme is to oxidize the H<sub>2</sub> produced by nitrogenase during the reduction of N<sub>2</sub> to NH<sub>3</sub>. *A. vinelandii* hydrogenase efficiently scavenges the H<sub>2</sub> produced in situ by nitrogenase. This efficiency is facilitated by the high affinity for H<sub>2</sub> (*K<sub>m</sub>* near 1 μM) and the low rate of the back-reaction (production of H<sub>2</sub>) (Seefeldt & Arp, 1986; Kow & Burris, 1984). As isolated, hydrogenase from *A. vinelandii* consists of two nonidentical subunits of about 65 000 and 35 000 molecular weight which are present in a 1:1 ratio to give a native molecular weight near 100 000. The enzyme also contains Ni and Fe in a 1:10–11 ratio (Seefeldt & Arp, 1986). EPR<sup>1</sup> and UV-vis spectroscopy indicate that the Fe is present in FeS centers, though the exact number and type are not known (Seefeldt, 1989).

Hydrogenase from *A. vinelandii* is typical of a number of hydrogenases isolated from physiologically distinct groups of microorganisms. For example, hydrogenases isolated from *Rhodobacter capsulatus*, *Alcaligenes eutrophus*, *Escherichia coli*, *Desulfovibrio gigas*, *Desulfovibrio baculatus*, *Thiocapsa roseopersicina*, and *Bradyrhizobium japonicum* all have similar subunit compositions and contain Ni and FeS centers

(Przybyla et al., 1991). The similarity among these NiFe hydrogenases is further reflected in their cross-reactivity to antibodies raised against individual hydrogenases (Kovacs et al., 1989). The structural genes coding for several of these NiFe hydrogenases have been sequenced, and they reveal a strong conservation in the locations of a number of amino acids, especially cysteines (the likely ligands to the FeS centers) and histidines as well as the amino acids flanking these cysteines and histidines (Przybyla et al., 1991).

It is of interest to determine the roles of each of the subunits in the oxidation of H<sub>2</sub> by these hydrogenases as well as the location and function of the metal centers. Nickel is apparently bound to the large subunit of the *D. baculatus* hydrogenase. <sup>77</sup>Se EPR (He et al., 1989b) and EXAFS (Eidsness et al., 1989) have revealed an interaction of the Ni with Se, which is found on selenocysteine [amino acid residue 493 on the large subunit (Voordouw et al., 1989)]. This selenocysteine is replaced by a conserved cysteine in other NiFe hydrogenases, leading to the suggestion that this cysteine binds Ni in these hydrogenases (Przybyla et al., 1991). However, analysis by proton-induced X-ray emission spectroscopy of the metal

<sup>1</sup> Abbreviations: EDTA, ethylenediaminetetraacetic acid; EPR, electron paramagnetic resonance; EXAFS, extended X-ray absorption fine structure; SDS, sodium dodecyl sulfate; SDS-PAGE, sodium dodecyl sulfate-polyacrylamide gel electrophoresis; TCA, trichloroacetic acid; Tris, tris(hydroxymethyl)aminomethane.

<sup>†</sup> This work was supported by U.S. Department of Energy Grant No. DEFGG-90ER20013 and the Oregon Agricultural Experiment Station.

\* To whom correspondence should be addressed.